UNIVERSITY OF CAMBRIDGE
Faculty of Economics

CAMBRIDGE WORKING PAPERS IN ECONOMICS

WANING IMMUNITY AND THE SECOND WAVE: SOME PROJECTIONS FOR SARS-CoV-2

Chryssi Giannitsarou | Stephen Kissler | Flavio Toxvaerd

Abstract

This paper offers projections of future transmission dynamics for SARS-CoV-2 in an SEIRS model with demographics and waning immunity. In a stylized optimal control setting calibrated to the USA, we show that the disease is endemic in steady state and that its dynamics are characterized by damped oscillations. The magnitude of the oscillations depends on how fast immunity wanes. The optimal social distancing policy both curbs peak prevalence and postpones the infection waves relative to the uncontrolled dynamics. Last, we perform sensitivity analysis with respect to the duration of immunity, the infection fatality rate and the planning horizon.

Reference Details

CWPE 20126
Published 18 December 2020

Key Words COVID-19, economic epidemiology, social distancing, waning immunity, demographics, infection control, SEIRS.
JEL Codes E61, I18

Website www.econ.cam.ac.uk/cwpe

WANING IMMUNITY AND THE SECOND WAVE: SOME PROJECTIONS FOR SARS-CoV-2 *

Chryssi Giannitsarou[†] Stephen Kissler[‡] Flavio Toxvaerd[§]

First draft: 2 June 2020;
Current draft: 22 September 2020

Abstract. This paper offers projections of future transmission dynamics for SARS-CoV-2 in an SEIRS model with demographics and waning immunity. In a stylized optimal control setting calibrated to the USA, we show that the disease is endemic in steady state and that its dynamics are characterized by damped oscillations. The magnitude of the oscillations depends on how fast immunity wanes. The optimal social distancing policy both curbs peak prevalence and postpones the infection waves relative to the uncontrolled dynamics. Last, we perform sensitivity analysis with respect to the duration of immunity, the infection fatality rate and the planning horizon.

JEL Classification: E61, I18.

Keywords: COVID-19, economic epidemiology, social distancing, waning immunity, demographics, infection control, SEIRS.

*We thank Andy Atkeson for constructive discussions, and our editor Pete Klenow and three anonymous referees for useful feedback and suggestions. We also benefited from conversations with Elisa Faraglia and Miltos Makris. The first draft of this paper was written under lockdown in April and May 2020. We thank our offspring Isabel and Nefeli for their patience and support during difficult times.

[†]Faculty of Economics, University of Cambridge and CEPR. Email: cg349@cam.ac.uk.

[‡]Harvard School of Public Health. Email: skissler@hsph.harvard.edu.

[§]Faculty of Economics, University of Cambridge. Email: fmot2@cam.ac.uk.

The 20th century witnessed a dramatic transition in the burden from infectious diseases. In the USA, the yearly mortality rate per 100,000 population fell from around 800 in the early 1900s to about 50 by mid-century (Armstrong et al., 1999, Hansen et al., 2016). These gains in public health were made possible by a series of significant innovations, not least by the development of treatments and vaccines. Since the 1950s, these mortality rates have remained relatively stable, despite increases in deaths due to diseases such as HIV/AIDS in the 1980s. This relative stability of mortality numbers over the past decades may have lead to complacency, with many advanced economies still ill-equipped to contain large-scale epidemics. Yet as is now clear, societies must confront the difficult question of how to best organize themselves in a world where new infectious diseases keep appearing and may remain endemic. A case in point is COVID-19, which is causing devastating health and economic effects around the world.

Much recent research on COVID-19 resorts to modelling the economic control of infection with variations of the classical SIR framework, in which recovery from the disease confers permanent immunity. Yet according to the WHO, *"There is currently no evidence that people who have recovered from COVID-19 and have antibodies are protected from a second infection."* This is important, because much of current policy is based on the assumption that herd immunity will eventually set in. The focus on getting through the first wave of the epidemic potentially leaves us exposed and unprepared to what comes after, if immunity wanes over time. At the time of writing, we still lack a vaccine or treatments that clearly reduce mortality from SARS-CoV-2, although there is cautious optimism that some pharmaceutical innovations may be on the horizon. Regardless, imperfect vaccine efficacy and incomplete coverage may alter the dynamics of the disease without fully eradicating it. Thus we may have to rely on some combination of non-pharmaceutical interventions and innovate on how we structure work and social life for the foreseeable future.

In this paper, we analyze optimal social distancing measures using a stylized yet flexible epidemic model with population turnover and waning immunity. We calibrate the model to the USA and perform comparative analysis with different assumptions about the waning period and disease-induced death rates. The calibrated epidemiological model has three important properties. First, with inflows to the population through births or migration, the disease becomes *endemic*. This means that if left uncontrolled, it will never be eradicated, in contrast to a closed population model in which recovery confers permanent immunity. Second, the path to the endemic steady state displays damped oscillations, which are intrinsic to the disease dynamics and unrelated to temporal forcing or time-varying behavior. Third, the periodicity of the oscillations and the speed of convergence to steady state depend on how fast immunity wanes. For this model, we find that it is optimal to have strict social distancing measures from the onset of the epidemic and which are continued for several months. These are then temporarily relaxed before being brought back at the start of the second wave, and subsequently maintained at a permanent moderate level. This policy achieves two goals: it suppresses and postpones the initial large infection wave, and delays all future waves as much as possible.

The fundamental difference between the models with permanent and waning immunity is that in the latter, the build-up of susceptibles happens faster, thereby generating additional waves of infection and deaths in the short and medium run. Waning immunity is thus similar to increasing the mortality of the disease relative to the case of permanent immunity. Optimal policy is sensitive to this difference and therefore prescribes stricter social distancing measures under waning immunity.

We also perform sensitivity analysis with respect to the speed at which immunity wanes and the infection fatality rate (IFR). For the calibrated benchmark and with immunity waning after one year, moderate changes in the two parameters change the policy in an intuitive manner; higher IFR and faster

loss of immunity both increase the severity of the disease and prompt stricter measures to be imposed. But for very fast loss of immunity or high IFR, there is a qualitative shift and the optimal policy no longer leads to an endemic steady state. Instead, significant and permanent social distancing is imposed from the outset, resulting in asymptotic eradication of the disease.

The recent literature on the economics of the COVID-19 epidemic is too vast to do justice in this space; for reference, we therefore mention just a few examples. Eichenbaum et al. (2020), Alvarez et al. (2020), Kaplan et al. (2020) and Krueger et al. (2020) all consider macroeconomic models in the SIR mold. In contrast, Toxvaerd (2019) and Rowthorn and Toxvaerd (2020) consider optimal control of an epidemic with reinfection in an SIS model. The model we consider here nests both the SIR and the SIS models, as it features both immunity and possible reinfection. Rachel (2020) considers the conditions under which a second wave can come about, in a simple closed population SIR setting.

1. A Model of Waning Immunity with Optimal Social Distancing

Time is continuous and for notational simplicity, we drop the time subscripts t from all time varying variables.

1.1. The Epidemic Model. The population is of size N. Susceptible individuals S become exposed to the disease by interacting with others who are either exposed E or infected I. This happens at rate $\beta\left(I+\varepsilon E\right)/N$, where $\beta>0$ is the rate of infection transmission upon contact with someone infectious, and $0<\varepsilon\leq 1$ allows for reduced infectiousness of those that are exposed but not symptomatic (Brauer and Castillo-Chavez, 2012). Exposed individuals transition to the infected state at some rate $\kappa>0$. Once infected, an individual recovers and transitions to recovered R at rate $\gamma>0$, and while in this state, enjoys immunity to new infection. Recovered individuals cannot become infected, but their immunity wanes over time and they transition back to the class of susceptibles at rate $\alpha\geq 0$. We allow for inflows of susceptible individuals into the population through births $\nu\geq 0$, for outflows through natural death at rate $\mu\geq 0$ from any health state and through disease-induced mortality at rate $\delta\geq 0$. Individuals in D died either from natural causes or from the disease. For any policy choice d, to be described below, the dynamics of the epidemic model are summarized by the following equations:

$$\dot{S}=\nu-(1-d)\beta\frac{\left(I+\varepsilon E\right)S}{N}+\alpha R-\mu S, \tag{1}$$

$$\dot{E}=(1-d)\beta\frac{\left(I+\varepsilon E\right)S}{N}-\left(\kappa+\mu\right)E, \tag{2}$$

$$\dot{I}=\kappa E-\left(\gamma+\delta+\mu\right)I, \tag{3}$$

$$\dot{R}=\gamma I-\left(\alpha+\mu\right)R, \tag{4}$$

$$\dot{N}=\nu-\mu N-\delta I, \tag{5}$$

$$\dot{D}=\delta I+\mu N, \tag{6}$$

for some initial states N_0, S_0, E_0, I_0 and R_0. We use the acronym SEIRS whenever $\alpha\neq 0$ (waning immunity) and SEIR when $\alpha=0$ (permanent immunity).

The model is closely related to the one presented by Kissler et al. (2020), but differs in some key aspects. First, we only consider the transmission of SARS-CoV-2 and do not model the transmission of other coronavirus strains that could induce cross-immunity. The evidence for cross-immunity between other coronavirus strains and SARS-CoV-2 is limited and is unlikely to play a major role in the epidemic dynamics discussed here. Furthermore, the present model allows for exposed individuals to transmit the virus, due to mounting evidence that pre-symptomatic transmission is key to the spread of SARS-CoV-2

(Li et al., 2020). Additionally, we introduce the policy instrument d, which we will discuss in more detail below.

We first discuss the dynamics without any policy intervention ($d = 0$) assuming a naive population. In the Online Appendix, we show that the uncontrolled dynamic system admits two steady states: a *disease-free* steady state and an *endemic* steady state. For any given parameterization, only one steady state is stable and stability is determined by the basic reproduction rate $\mathcal{R}_0$. For calibrated SARS-CoV-2 parameters, we show that the stable steady state for the uncontrolled system with $d = 0$ is the endemic one. This is true even with permanent immunity, because $\mathcal{R}_0$ does not depend on α and is always larger than one. The dynamics of the system exhibit damped oscillations and the periodicity of these depends on the key parameter α: as immunity wanes faster, the consecutive waves arrive faster. Intuitively, the damped oscillations are generated because both demographics and waning immunity replenish the pool of susceptibles, creating the potential for additional waves. Births constitute a direct source of susceptibles, while waning immunity speeds up this accumulation by drawing on the pool of recovered people. Thus waning immunity causes additional waves to appear earlier than they would have under permanent immunity. With permanent immunity, it can take very long before enough births accumulate to create another spike in prevalence.[1] We also emphasize that in the SEIR model without demographics the disease always dies out over time and does not display any oscillatory behavior, while the SEIR with demographics may have oscillatory behavior, depending on parameters (see Online Appendix). Thus the seemingly simple addition of births and deaths to the model has important implications for the behavior of the disease dynamics.

Next, we consider a simple non-optimizing policy of treating d as a *constant parameter* that reduces the contact rate between susceptible and infectious individuals, and can be interpreted as a measure of social distancing, i.e. capturing any broad contact-reducing measure that can be scaled from a complete lockdown of all social activity $d = 1$, to a laissez-faire outcome without any restrictions at all $d = 0$. The system still exhibits two steady states, one endemic and one disease-free, and only one can be stable for each set of parameters. In the Online Appendix, we show that the endemic steady state remains stable whenever distancing is below a threshold level $\tilde{d} \equiv 1 - 1/\mathcal{R}_0$, while the disease is asymptotically eradicated for $d > \tilde{d}$. Although not optimal, this policy experiment is useful for interpreting the dynamics of the optimal social distancing policy.

1.2. The Economic Model with Optimal Social Distancing. We assume that susceptible, exposed, infected, recovered and deceased individuals earn instantaneous flow payoffs y_S, y_E, y_I, y_R and y_D, respectively. Interpreting this model as a reduced-form macroeconomic framework, these parameters can be thought of as income generated per each type of individual in the economy. We assume that

$$y_S = y_E \geq y_R > y_I > y_D = 0. \tag{7}$$

This captures the following: first, exposed individuals are not yet symptomatic and thus have the same income as those who are susceptible. Second, infected individuals experience a decrease in income from becoming infected, e.g. due to a drop in productivity, and an increase once they recover. Last, deaths constitute a welfare loss counted as the opportunity cost of income earned while still alive.

Given some planning horizon, a benevolent utilitarian social planner now *chooses* the degree of social distancing $0 \leq d \leq 1$ at each moment to optimally reduce the infectiousness parameter to $(1 - d)\beta$ and

[1] In practice, this may take several decades. Conceivably, the nature of the disease may change over such long time horizons, as well as react to external factors like pharmeceutical innovations, policy and behavioral responses.

solve the problem

$$\max_{d\in[0,1]} \left\{ \int_0^T e^{-\rho t} \left(y_S S(t) + y_E E(t) + y_I I(t) + y_R R(t) - \frac{\theta}{2} d(t)^2 \right) dt + \int_T^\infty e^{-\rho t} y N(t) dt \right\}, \tag{8}$$

subject to (1)-(6), initial conditions N_0, S_0, E_0, I_0, R_0, where $\theta d^2/2$ with $\theta > 0$ is the aggregate cost of social distancing.

The planner's objective has two parts. Until time T, the planner trades off costs and benefits of infection control. At time T, the nature of the problem changes and the infection ceases to be a concern to the planner: from T onwards, every individual earns $y \equiv y_S$ per instant and there are no more expenses of social distancing.[2] For any finite horizon $T < \infty$, this situation can be interpreted as one in which radical pharmaceutical innovations make social distancing obsolete at a known point in time. E.g., Acemoglu et al. (2020) assume that at some finite time T, perfect and costless vaccines and treatments become simultaneously available. Our formulation ensures that the value of lives beyond time T still features in social welfare and thus influence optimal policy. As $T \to \infty$, our model approximates an infinite horizon model, which is nevertheless compatible with the potential arrival of pharmaceutical interventions, since vaccine coverage may be incomplete, some people may be reluctant to vaccinate themselves or their children, or vaccines may not confer perfect protection and wane in effect over time. Thus the infinite horizon setting can be thought of as the worst-case scenario in a world in which vaccines eventually become available, but do not completely eradicate the disease.

In the Online Appendix, we derive and state the necessary conditions for an optimal policy and show that it takes the form

$$d^* = \max\left\{0,\ \min\left\{1,\ \left(\frac{e^{\rho t}}{\theta}(\lambda_S - \lambda_E)\beta\frac{(I+\varepsilon E)S}{N}\right)^{1/\eta}\right\}\right\}, \tag{9}$$

where λ_S and λ_E are the costate variables for constraints (1)-(2) respectively. The optimal d^* equates the marginal cost of social distancing with its marginal benefit. Social distancing reduces additional transition from susceptible to infectious at rate $\beta(I+\varepsilon E)S/N$. This increases social welfare at rate $(\lambda_S - \lambda_E)$, which is the net cost of additional exposed people in terms of shadow prices.

2. Projected Epidemic Scenarios

The dynamics under optimal control are solved for numerically by using a forward-backward sweep method, as described in Lenhart and Workman (2007), with details given in the Online Appendix.

2.1. Calibration. We calibrate our model to the USA at weekly frequency. As the benchmark case, we set the planning horizon to $T = 100$ years. We measure the population in millions of individuals, so that the initial conditions for the model are $N_0 = 330$. We assume that initially, there are one in ten million individuals infected, so $I_0 = 0.000033$ and that $E_0 = 3 \times I_0$, i.e. that there are initially some exposed individuals who are still presymptomatic. These numbers are taken from Atkeson (2020).

The epidemic parameters are taken from Kissler et al. (2020) and amended with more up-to-date estimates where necessary. We set $\nu = 3.8/52$, since there are approximately 3.8 million babies born in the USA per year. The natural death rate is set to $\mu = 1/(80 \times 52)$ to capture an average expected life span of 80 years. The transition rate from infected to recovered is set to $\gamma = 7/14$, capturing estimates

[2] Implicit in this formulation is the assumption that a period of life is valued at the income generated by an individual in the same period. In a recent paper, Hall, Jones and Klenow (2020) explain that empirically the 'value of a year of life' can be up to six times the annual consumption of a representative individual.

that it can take up 14 days for infected individuals to recover. We set $\beta = 3 \times \gamma$, to match the usual calibration which assumes that the basic reproduction rate for SARS-CoV-2 is somewhere between 2.5 and 3.5. The literature suggests that the median incubation period is five days, so we set $\kappa = 7/5$ (see Kissler et al., 2020).

The parameter ε captures the infectivity of individuals that are exposed but not yet symptomatic. We assume as a benchmark that $\varepsilon = 0.5$ (Davies et al., 2020) and note that the results are not very sensitive to small changes in this parameter. The parameter δ captures the death rate of infected individuals due to SARS-CoV-2 . Estimates for the IFR for SARS-CoV-2 vary. Research articles with data from China (Verity et al., 2020), France (Salje et al., 2020), Switzerland (Perez-Saez et al., 2020) and Iceland (Gudbjartsson et al., 2020) estimate the IFR to 0.66%, 0.7%, 0.64% and 0.3% respectively. A meta-analysis of estimated IFRs from July 2020 suggests a point estimate of 0.68% (Meyerowitz-Katz and Merone, 2020). On this background, we use IFR of 0.65% as the benchmark value and set $\delta = 0.0065 \times \gamma$.

Next, we assume as a benchmark that $\alpha = 1/52$, so that immunity wanes in one year after infection. At the time of writing, the duration of immunity for SARS-CoV-2 is still uncertain. Immunity to other coronaviruses is known to decline over time: in one study, volunteers were intentionally infected with a coronavirus strain (229E) that usually causes common cold symptoms. Many participants were successfully re-infected with the same virus one year later (Callow et al., 1990). Other mild coronaviruses often have immunity that wanes between less than one year to two years after infection (Kissler et al., 2020 and Galanti and Shaman, 2020). The duration of immunity for SARS and MERS have been estimated to be about two and three years, respectively (Mo et al., 2006 and Payne et al., 2016). SARS-CoV-2 has not been circulating long enough to definitively conclude how long immunity lasts. However, recent studies have shown that one key element of the immune response, the B cell response, does wane substantially in the weeks following infection (Seow et al., 2020). There is also at least one confirmed case of re-infection with SARS-CoV-2 from Hong-Kong, as reported in To et al. (2020) and a case of re-infection in Nevada, USA is currently being investigated. While at the moment it appears that immunity lasts at least 4 months, as suggested by the comprehensive study from Iceland by Gudbjartsson et al. (2020), further longitudinal studies are needed to determine the mean duration of immunity.

Turning to the economic parameters, we normalize the production per individual to a unit, and set $y_S = y_E = y_R = 1$ and $y_I = 0.9$. We set $\theta/2 = 330 \times 0.165$ so that the cost of distancing per individual of the initial population is consistent with the magnitudes reported by Strong and Wellbourn (2020), who estimate that the decline in income per capita due to social distancing across a variety of sectors and lockdown scenarios is between 4.6 and 25.6%. The parameter values we use in our simulations are listed in Table 1 of the Online Appendix.

For these parameters, the stable steady state is endemic and the path to steady state exhibits damped oscillations. The constant threshold parameter $\tilde{d}$ above which the disease is asymptotically eradicated is 71.54%.

2.2. The effects of optimal social distancing. Our simulations are based on $T = 100$ years, however for clarity of exposition the figures show only the first six years from the onset of the epidemic, which is a relevant time frame for practical policy design in the short and intermediate run. Figures 1 and 2 show the disease dynamics for the SEIR and SEIRS models respectively, for the benchmark calibration. In each of these, the top four panels show the dynamics of both the uncontrolled epidemic (dotted lines) and those under optimal social distancing (solid lines). The bottom left panel shows the

differences in cumulative disease-induced deaths and the bottom right panel the path of optimal social distancing.

We first describe how the dynamics of the two uncontrolled models compare. The uncontrolled SEIRS dynamics initially share some properties with the uncontrolled SEIR counterparts. Susceptibles initially decrease while recovered individuals increase. Infection first picks up and then decreases, an effect of susceptibles becoming scarcer and some herd immunity setting in. In the SEIRS model, because immunity wanes over time, a large number of recovered individuals that accumulate at the initial stages of the epidemic quickly migrate back to the pool of susceptibles, forming the basis of an additional wave of infection. This new reservoir of susceptibles creates a smaller second wave of infection, with the concomitant effects on susceptibles and recovered individuals. This is seen as a second wave of infections, peaking about one year after the first wave. In the SEIR model, this process takes much longer: the number of susceptibles actually increases very slowly after the first wave and creates a second smaller wave of infections, about 53 years after the peak of the first wave (see Online Appendix).

Next, we turn to the optimal social distancing policy. In the SEIR framework, the path of optimal social distancing in the intermediate run looks a lot like the policies that have been used in many countries to control the epidemic: in the beginning there is little social distancing, which then sharply increases as the first peak approaches, and then sharply decreases as infected individuals recover, gain immunity and remain healthy thereafter. Around the peak, sometime in week 19 after the epidemic starts, optimal social distancing in the SEIR framework reaches its maximum level of 33%, however this lasts for a short period of time, and is essentially phased out by week 35. The effects of the social distancing policy are a flattened curve and a slightly lengthier epidemic. The number of infected individuals under the optimal policy at the peak of the epidemic is about 23% smaller than that in the uncontrolled model. Once the first wave has passed, social distancing is kept at a very low level for about five decades, when a second wave in infection occurs. At this point (and similarly for subsequent waves), social distancing is temporarily and slightly intensified. In the SEIRS framework, the optimal social distancing policy is quite different in the short and medium run. Significant restrictions at 54% distancing are imposed from the very start and maintained for the best part of one year. After that, restrictions are temporarily phased out until the second wave approaches, at which point control efforts are intensified and social distancing is again increased to 20%. Social distancing eventually settles on a permanent moderate level of 12%.

Some comments are in order. First, even under optimal social distancing, the different trajectories remain non-monotone and so it is part of the optimal policy to allow infection to increase temporarily. While social distancing clearly suppresses peak prevalence in both settings, under waning immunity it also serves to delay the time of the first and subsequent waves. Under permanent immunity, the timing of the first wave is almost unchanged, although the magnitude is of course decreased relative to the uncontrolled dynamics.

Second, for both models the optimal policy is such that the disease remains endemic, since the optimal social distancing never reaches the threshold of $\tilde{d} = 71.54\%$. It is simply too costly for society to eradicate the disease, given the parameters that characterize it. Instead, the optimal policy is a permanent low level management of the disease with social distancing of approximately 12%. This result clearly depends both on the parameters that describe the epidemic, e.g. the IFR, the speed of waning immunity, etc., and on the configuration of the optimal policy problem, i.e. the discount rate, how costly social distancing is, how much income is lost when individuals are infected and how much value lost lives have. As we will show in the next section, when the disease becomes very deadly (high δ) or immunity wanes very

fast (high α), the optimal policy may be to steer the system to the disease-free steady state. In practice, this entails a very high level of social distancing at or above $\tilde{d}$ and eradicates the disease asymptotically.

Third, the optimal suppression policies under the two models are qualitatively very different at the early stages of the epidemic. With permanent immunity, the best policy is to delay intervention for several weeks until infection picks up and then impose strict restrictions on social interaction. In contrast, with waning immunity, it is optimal to immediately impose strict measures and keep them in place for a period of about a year. From the perspective of a policy maker, it is therefore important to have a sense of which of the two models best describes the ongoing COVID-19 pandemic. While it is of course impossible to know at this early stage whether immunity wanes in the medium run, various medical studies suggest that the relation of SARS-Cov-2 to other coronaviruses with waning immunity may be a good indicator for this.

Fourth, when comparing the difference in cumulative disease-induced deaths between controlled and uncontrolled models, we see that after six years there are approximately $102,120$ deaths difference for the SEIR model, while for the SEIRS model, the optimal policy saves the lives of approximately 1.423 million people.

Last, the figures for the two models suggest that the numbers of infected individuals at about four months into the epidemic are substantially higher than those currently projected for the USA.[3] A variety of factors may contribute to explaining this. First, epidemic parameters such as the IFR, the incubation period, or the infectivity of presymptomatic individuals are not yet fully understood. In practice, they may differ from the ones used here. Second, it is thought that there are many more cases of infected individuals than those confirmed by testing, since a large fraction of the population are tested only when they exhibit symptoms; numerous reports since February 2020 suggest that more than one third of the world's population could end up being infected. In a recent unpublished paper, Swanson and Cossman (2020) suggest that the estimated number of cases in the USA is somewhere between 7.5 and 14 times higher than the reported number of infected cases. At the time of writing of the first draft, on June 1, 2020, there were about 1.8 million reported/confirmed cases, which implies that the actual number of cases of infection may currently be between 13.5 and 25 million individuals. Our benchmark calibration generates numbers of comparable order of magnitude for weeks 16 and 17 of the epidemic, for the uncontrolled model. Last, the calculation of the optimal social distancing policy does not factor in any spontaneous social distancing that individuals may engage in (see Toxvaerd, 2020).

3. Sensitivity Analysis

3.1. Waning immunity. Figure 3 shows the prevalence of infection and the optimal social distancing policy for $\alpha = 1/26,\ 1/52$ (benchmark), $1/104$ and 0 (SEIR). Infection prevalence in the uncontrolled models always exhibit a first peak 19 weeks into the epidemic, and these first peaks are almost identical irrespective of the waning period. As the first wave subsides, a new wave occurs with arrival time that depends on how quickly immunity wanes and a peak of lower size, that is smaller for longer-lasting immunity. As α approaches zero, we revert to the SEIR model, which does not generate a second wave within intermediate time horizons. Under optimal social distancing, these dynamics look qualitatively similar to those in the uncontrolled system. With waning immunity, the controlled infection dynamics display damped oscillations, a behavior inherited from the underlying epidemic model. But the optimal policy has two additional effects: all waves are suppressed and they are pushed forward in time.

[3] Our assumption is that the epidemic in the USA is initiated some time in early February, which means that at the time of writing of the first draft of this paper in late May 2020, the USA was in week 16-17 of the epidemic.

In the bottom panel, we show the optimal social distancing policy for the different values of α. As α decreases, the optimal policy prescribes an immediate and substantial reduction in social interactions lasting from three to six months, followed by intermittent periods of heightened control in order to manage subsequent waves of infection. We also observe that aggressive social distancing at the start of the epidemic for larger α pushes the first peaks forward. This happens because as immunity wanes more rapidly, the policy maker hopes to suppress as many of the potential peaks as possible before the end of the planning horizon. Finally, as immunity wanes very fast, for $\alpha = 1/26$, there is a major shift in optimal policy. The effective disease mortality and loss of income now become so high that the optimal policy steers the system away from the endemic steady state, and towards asymptotic eradication of the disease. In the lower panel, we note that optimal social distancing in this case approaches the level $\tilde{d} = 71.54\%$, the threshold that ensures asymptotic eradication. In this disease-free steady state, it would never be optimal to impose distancing at a higher level than $\tilde{d}$, as distancing is costly and this level ensures that the disease is approximately eradicated. In the Online Appendix we also report the numbers of deaths after 6 years and at the end of horizon for each case analyzed.

3.2. Disease-induced mortality. In Figure 4, we present the dynamics of infected individuals for three values of the IFR, namely 0.3%, 0.65% (benchmark) and 1.2%. The effects of these differences in the death rate δ are imperceptible for the uncontrolled system (top panel). However, the controlled dynamics of infected individuals differ significantly for the three parameters. At the end of six years, the reduction in cumulative disease-induced deaths relative to the uncontrolled model is 158,010, 1.423 million and 17.476 million people for IFRs 0.3%, 0.65% and 1.2% respectively. Thus the optimal policy can make a substantial difference in terms of the total number of lives saved.

The optimal policy for social distancing is intuitive: the higher the IFR is, the stricter are the measures for social distancing at the start of the epidemic, and the longer they last. Following the initial relaxation of the measures, the social distancing increases again to suppress the second wave, in a monotonic way. As was the case with very fast immunity waning, when the IFR is sufficiently high, e.g. 1.2%, there is a qualitative shift in optimal policy and the system is steered towards asymptotic eradication rather than to the endemic steady state. The intuition for this mirrors that for the case of high α. In fact, this observation suggests a strong link between the effective mortality rate of the disease and the degree of waning immunity: when immunity is not permanent, individuals are repeatedly subject to infection and the risk of death. This means that the IFR may be a poor measure of the overall mortality across the epidemic. It also shows that if policy makers conduct cost-benefit analysis based on estimated IFRs and erroneously assume that immunity is permanent, they may be seriously underestimating the magnitude of the disease burden.

3.3. Planning horizon. We close by considering the cases of $T = 2,\ 4,\ 6$ years and compare them with the long horizon case $T = 100$ years, shown in Figure 5. To interpret the different effects, we note that in short horizons, optimal policy has two goals. First, it directly trades off costs of social distancing with disease-induced costs, namely lost income and increased mortality over the time interval $[0, T]$. Second, by influencing the number of deaths over the planning horizon, the optimal policy indirectly affects the size of the population and thus the initial condition for the post-planning value of life, captured by the salvage value at T. The shorter the horizon is, the more weight is given to the second goal, while when $T \to \infty$, this second concern becomes negligible due to discounting. It therefore has little effect on the optimal policy away from the end time.

When $T \to \infty$, the optimal policy consists of intense initial levels of social distancing to suppress and

postpone the first large peak, and subsequent smaller and sustained levels in social distancing to manage later peaks. But as the horizon becomes finite and shorter, the presence of the salvage value becomes so important that all else equal, the planner now has a strong incentive to maximize the number of people alive at date T, thus reaping maximal benefits from the lives after time T. In the simulations, this effect shows as a substantial ramping-up of social distancing towards the end of the planning horizon. For shorter planning horizons both the effort for peak reduction and the effort to increase end of horizon survivors are present in the optimal policy. As the planning horizon increases, the policy responds more to the disease dynamics, reflected in the varying intensity of social distancing seen in the graphs for $T = 4, 6$. In contrast, for the case $T = 2$, the horizon becomes so short that waning immunity has less effect, while increasing the number of survivors becomes the paramount policy concern.

4. Conclusion

In this paper, we study optimal social distancing measures to contain COVID-19. Relative to the baseline closed-population model with permanent immunity, we make two important departures. First, we add demographics to the epidemic model and second, we allow for the possibility of waning immunity. These two features interact in interesting ways. We find that for the parameters describing SARS-CoV-2 the population turnover is sufficient for the disease to become endemic, ceteris paribus. The path to the steady state involves damped oscillations in the underlying epidemic model, which is in turn reflected in the optimal path of social distancing and disease prevalence. We also find that the periodicity of the damped oscillations depends on how fast immunity wanes. For our benchmark scenario where immunity wanes after one year, the system approaches the steady state fast and most oscillations occur within the first six years of the epidemic.

Damped oscillations are a well-known property of SIR-type models with demographics (e.g. Keeling and Rohani, 2008) and characterizes infectious diseases such as measles (Grenfell et al., 2001 and Grenfell and Bjørnstad, 2005), syphilis (Grassley et al., 2005) and smallpox (Greer et al., 2020). Measles is an interesting example, as it is vaccine preventable and recovery induces permanent immunity. Grenfell et al. (2001) show that measles not only displays damped oscillations when uncontrolled, but has remained endemic even in the post-vaccine era. To date, smallpox is the only known vaccine preventable infectious disease that has been completely eradicated. As argued by Grenfell and Bjørnstad (2005), nonlinear interactions between pathogens and the human immune system can generate periodicity in disease incidence and prevalence, without the need for temporal forcing or behavioral changes. This turns out to be the case in our model for SARS-CoV-2.

As a practical matter, it is too early to tell whether immunity to reinfection is permanent or not. This can only be established through longitudinal studies, which may take years. Experience from related viruses suggest that there is a realistic prospect that some waning may take place, in which case societies may be forced to find ways to live with the disease, rather than return to pre-epidemic norms. For this reason, it is important to start planning for that possibility now. The present research is a first step in this direction and we show that ignoring demographics, or relying on the emergence of permanent immunity, may give incomplete policy recommendations.

Our analysis applies more broadly and offers insights for how to implement optimal disease control whenever new infectious diseases appear. Many infections only induce temporary immunity, making their control substantially more difficult and underscoring the importance of using epidemic models that capture the long-term dynamics that waning immunity implies. Pandemic influenza strains, for example, normally enter into circulation with seasonal influenza viruses and continue to cause disease

well after the declared pandemic has ended. Active tuberculosis disease can recur periodically over the course of an infection and re-infection with new strains is common in high-prevalence settings. Some sexually transmitted infections, such as gonorrhea, induce virtually no immunity. For SARS-CoV-2, a model with waning immunity aligns with the most up-to-date information about the virus' immunogenic characteristics. Other illnesses require models with different structures to capture the specific epidemiological characteristics that affect long-term transmission dynamics. No model is able to capture all elements of a disease's transmission patterns, yet some choices are clearly better than others; one would never use a traditional permanently-immunizing SIR model to describe the dynamics of gonorrhea, for example. For long-term economic planning, it is imperative to work with models that capture key characteristics of the disease in question.

References

[1] Alvarez, F., D. Argente and F. Lippi (2020). A Simple Planning Problem for COVID-19 Lockdown, *NBER Working Paper* 26981.

[2] Armstrong, Gregory L., Laura A. Conn and Robert W. Pinner (1999). Trends in Infectious Disease Mortality in the United States During the 20th Century, *Journal of the Americal Medical Association*, 281(1), 61-66.

[3] Atkeson, A. (2020). What Will Be the Economic Impact of COVID-19 in the US? Rough Estimates of Disease Scenarios, *NBER Working Paper* 26867.

[4] Brauer, F. and C. Castillo-Chavez (2012). Mathematical Model in Population Biology and Epidemiology, *Springer*.

[5] Brock, W. A. and D. Starrett (2003): Managing Systems with Non-convex Positive Feedback, *Environmental and Resource Economics*, 26(4): 575-602.

[6] Brock, W. A. and W. D. Dochert (1983). The Generalized Maximum Principle, *Social Systems Research Institute Workshop Series*, University of Wisconsin.

[7] Callow, K. A., H. F. Parry, M. Sergeant and D. A. Tyrrell (1990). The Time Course of the Immune Response to Experimental Coronavirus Infection of Man, *Epidemiology and Infection*, 105(2), 435–446. doi: 10.1017/s0950268800048019.

[8] Davies, N.G., P. Klepac, Y. Liu, et al. (2020). Age-Dependent Effects in the Transmission and Control of COVID-19 Epidemics, *Nature Medicine* 26, 1205-1211. https://doi.org/10.1038/s41591-020-0962-9.

[9] Davies, N.G., P. Klepac, Y. Liu, K. Prem, M. Jit, CMMID COVID-19 working group, R. M. Eggo (2020). Age-Dependent Effects in the Transmission and Control of COVID-19 Epidemics, unpublished manuscript, medRxiv doi: https://doi.org/10.1101/2020.03.24.20043018.

[10] Deissenberg, C., G. Feichtinger, W. Semmler and F. Wirl (2004). Multiple Equilibria, History Dependence and Global Dynamics in Intertemporal Optimization Problems, in Barnett et al. (2004). Economic Complexity, Non-Linear Dynamics, Multi-Agents Economies, and Learning, International Symposia in Economic Theory and Econometrics, *Elsevier*.

[11] Eichenbaum, M., S. Rebelo and M. Trabrandt (2020). The Macroeconomics of Epidemics, *NBER Working Paper* 26882.

[12] Galanti, M. and J. Shaman (2020). Direct observation of repeated infections with endemic coronaviruses, *Journal of Infectious Diseases*, doi:10.1093/infdis/jiaa392.

[13] Grassly, Nicholas C., Christophe Fraser and Geoffrey P. Garnett (2005). Host Immunity and Synchronized Epidemics of Syphilis Across the United States, *Nature*, 433, 417-421.

[14] Greer, Meredith, Raj Saha, Alex Gogliettino, Chialin Yu and Kyle Zollo-Venecek (2020). Emergence of Oscillations in a Simple Epidemic Model with Demographic Data, *Royal Society Open Science*, 7(1), https://doi.org/10.1098/rsos.191187.

[15] Grenfell, B. T., O. N. Bjørnstad and J. Kappey (2001). Travelling Waves and Spatial Hierarchies in Measles Epidemics, *Nature*, 414, 716-723.

[16] Grenfell, Bryan and Ottar Bjørnstad (2005). Epidemic Cycling and Immunity, *Nature*, 433, 366-367.

[17] Gudbjartsson, D.F., G.L. Norddahl and P. Melsted et al. (2020). Humoral Immune Response to SARS-CoV-2 in Iceland, *The New England Journal of Medicine,* DOI: 10.1056/NEJMoa2026116.

[18] Hall, R. E., C. Jones and P. Klenow (2020). Trading Off Consumption and COVID-19 Deaths. *Federal Reserve Bank of Minneapolis, Quarterly Review*, 42(1).

[19] Hansen, Victoria, Eyal Oren, Leslie K. Dennis and Heidi E. Brown (2016). Infectious Disease Mortality Trends in the United States, 1980-2014, *Journal of the Americal Medical Association*, 316(20), 2149-2151.

[20] Kaplan, G., B. Moll and G. Violante (2020). The Great Lockdown and the Big Stimulus: Tracing the Pandemic Possibility Frontier for the U.S., *CEPR Discussion Paper 15256.*

[21] Keeling, Matt J. and Pejman Rohani (2008). Modeling Infectious Diseases, *Princeton University Press.*

[22] Kissler, S. M., C. Tedijanto, E. Goldstein, Y. H. Grad and M. Lipsitch (2020). Projecting the Transmission Dynamics of SARS-CoV-2 through the Postpandemic Period, *Science*, 368 (6493), 860–686. doi: 10.1126/science.abb5793

[23] Krueger, D., H. Uhlig and T. Xie (2020). Macroeconomic Dynamics and Reallocation in an Epidemic, *NBER Working Paper* 27047.

[24] Lenhart, S. and J. T. Workman (2007). Optimal Control Applied to Biological Models. Mathematical and Computational Biology Series, *Chapman & Hall/CRC*, London.

[25] Li, R., S. Pei, B. Chen, Y. Song, T. Zhang, W. Yang, and J. Shaman (2020). Substantial undocumented infection facilitates the rapid dissemination of novel coronavirus (SARS-CoV-2). Science, 368 (6490), 489-493. doi: 10.1126/science.abb3221

[26] Meyerowitz-Katz, G. and L. Merone (2020). A systematic review and meta-analysis of published research data on COVID-19 infection-fatality rates, medRxiv 2020.05.03.20089854; doi: https://doi.org/10.1101/2020.05.03.20089854.

[27] Mo, H., Zeng, G., Ren, X., Li, H., Ke, C., Tan, Y., Cai, C., Lai, K., Chen, R., Chan-Yeung, M. And Zhong, N. (2006), Longitudinal profile of antibodies against SARS-coronavirus in SARS patients and their clinical significance. *Respirology*, 11: 49-53. doi:10.1111/j.1440-1843.2006.00783.x

[28] Javier Perez-Saez, Stephen A Lauer, Laurent Kaiser, Simon Regard, Elisabeth Delaporte, Idris Guessous, Silvia Stringhini, Andrew S Azman, et al. (2020). Serology-informed estimates of SARS-CoV-2 infection fatality risk in Geneva, Switzerland, *The Lancet Infectious Diseases*, ISSN 1473-3099, https://doi.org/10.1016/S1473-3099(20)30584-3.

[29] Payne, D. C., Iblan, I., Rha, B., et al. (2016). Persistence of Antibodies against Middle East Respiratory Syndrome Coronavirus. *Emerging Infectious Diseases*, 22(10), 1824-1826. https://dx.doi.org/10.3201/eid2210.160706.

[30] Rachel, Łukasz (2020): The Second Wave, *mimeo.*

[31] Rowthorn, R. and F. Toxvaerd (2020). The Optimal Control of Infectious Diseases Via Prevention and Treatment, *Cambridge-INET Working Paper Series* No: 2020/13.

[32] Salje, H., C. Tran Kiem, N. Lefrancq, N. Courtejoie, P. Bosetti, J. Paireau, A. Andronico, N. Hoze, J. Richet, C-L. Dubost, Y. Le Strat, J. Lessler, D. Levy-Bruhl, A. Fontanet, L. Opatowski, P-Y. Boelle, S. Cauchemez (2020). Estimating the burden of SARS-CoV-2 in France, *Science*, 13 May 2020, doi: 10.1126/science.abc3517.

[33] Seow, J., C. Graham, B. Merrick et al. (2020). Longitudinal evaluation and decline of antibody responses in SARS-CoV-2 infection. Unpublished manuscript, medRxiv 2020.07.09.20148429; doi: https://doi.org/10.1101/2020.07.09.20148429.

[34] Strong, A. and J. W. Welburn (2020). An Estimation of the Economic Costs of Social-Distancing Policies, Research Report RR-A173-1, *RAND Corporation.*

[35] Swanson, D. and R. Cossman (2020). A Simple Method for Estimating the Number of Unconfirmed COVID-19 Cases in a Local Area that Includes a Confidence Interval: A Case Study of Whatcom County, Washington, unpublished manuscript, medRxiv, doi: 10.1101/2020.04.30.20086181.

[36] To, K. K. W, I. Fan-Ngai Hung, J. D. Ip, et al. (2020). COVID-19 re-infection by a phylogenetically distinct SARS-coronavirus-2 strain confirmed by whole genome sequencing, *Clinical Infectious Diseases*, https://doi.org/10.1093/cid/ciaa1275.

[37] Toxvaerd, F. (2019). Rational Disinhibition and Externalities in Prevention, *International Economic Review*, 60(4), 1737-1755.

[38] Toxvaerd, F. (2020). Equilibrium social Distancing, *Cambridge-INET Working Paper Series* No: 2020/08.

[39] Verity, R., L. C. Okell, I. Dorigatti, P. Winskill, C. Whittaker, N. Imai, G. Cuomo-Dannenburg, H. Thompson, P. G. T. Walker, H. Fu, A. Dighe, J. T. Griffin, M. Baguelin, S. Bhatia, A. Boonyasiri, A. Cori, Z. Cucunube, R. FitzJohn, K. Gaythorpe, W. Green, A. Hamlet, W. Hinsley, D. Laydon, G. Nedjati-Gilani, S. Riley, S. van Elsland, E. Volz, H. Wang, Y. Wang, X. Xi, C. A. Donnelly, A. C. Ghani, N. M. Ferguson (2020). Estimates of the Severity of Coronavirus Disease 2019: A Model-Based Analysis, *The Lancet Infectious Diseases*, 20(6), 669-677, https://doi.org/10.1016/S1473-3099(20)30243-7.

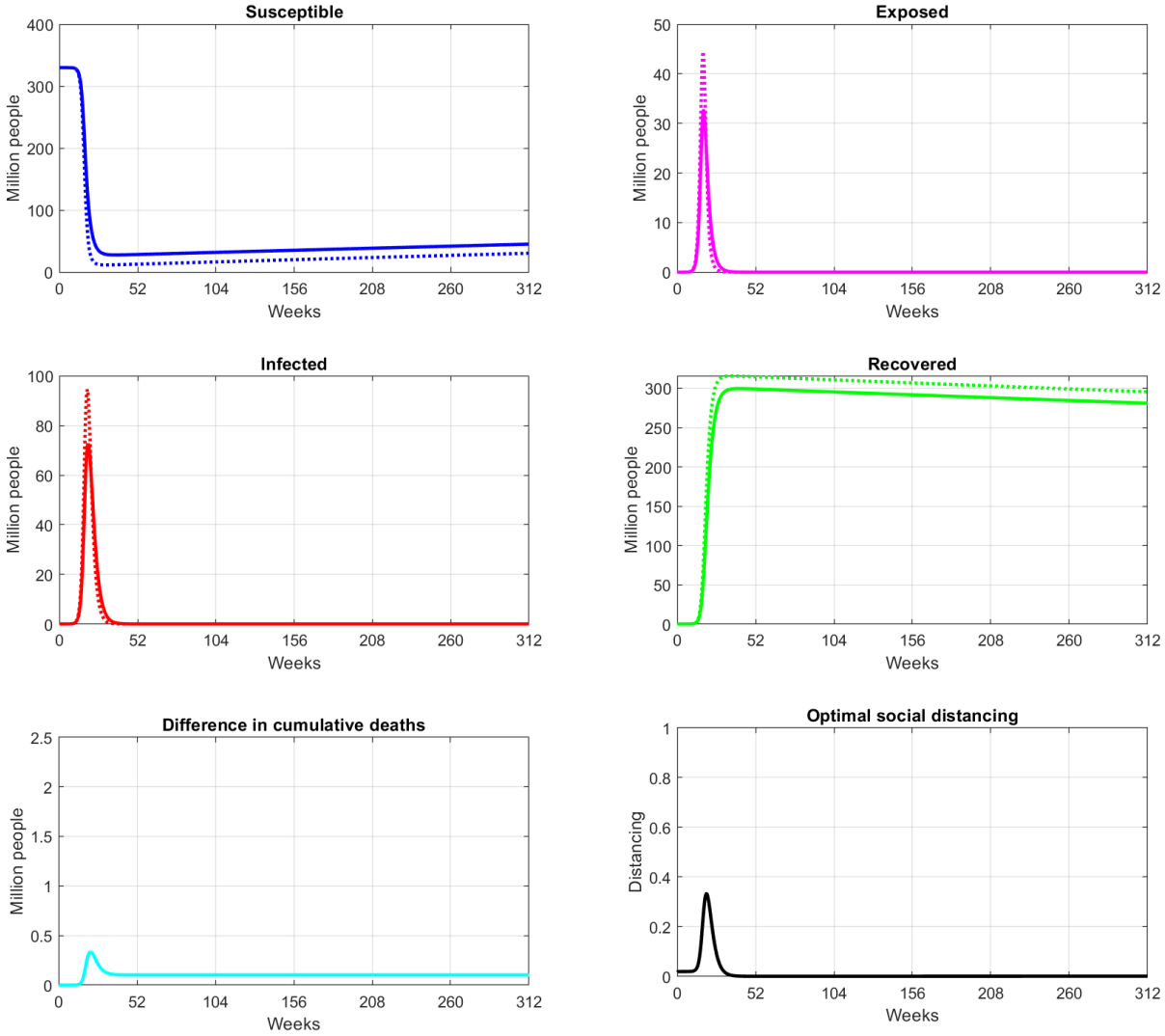

Figure 1: Dynamics for the SEIR model ($\alpha = 0$) under the benchmark parameterization. Dotted lines: dynamics under uncontrolled (epidemic) model. Solid lines: dynamics under optimal social distancing. Lower left panel: difference in cumulative disease-induced deaths under controlled and uncontrolled dynamics. Lower right panel: optimal social distancing.

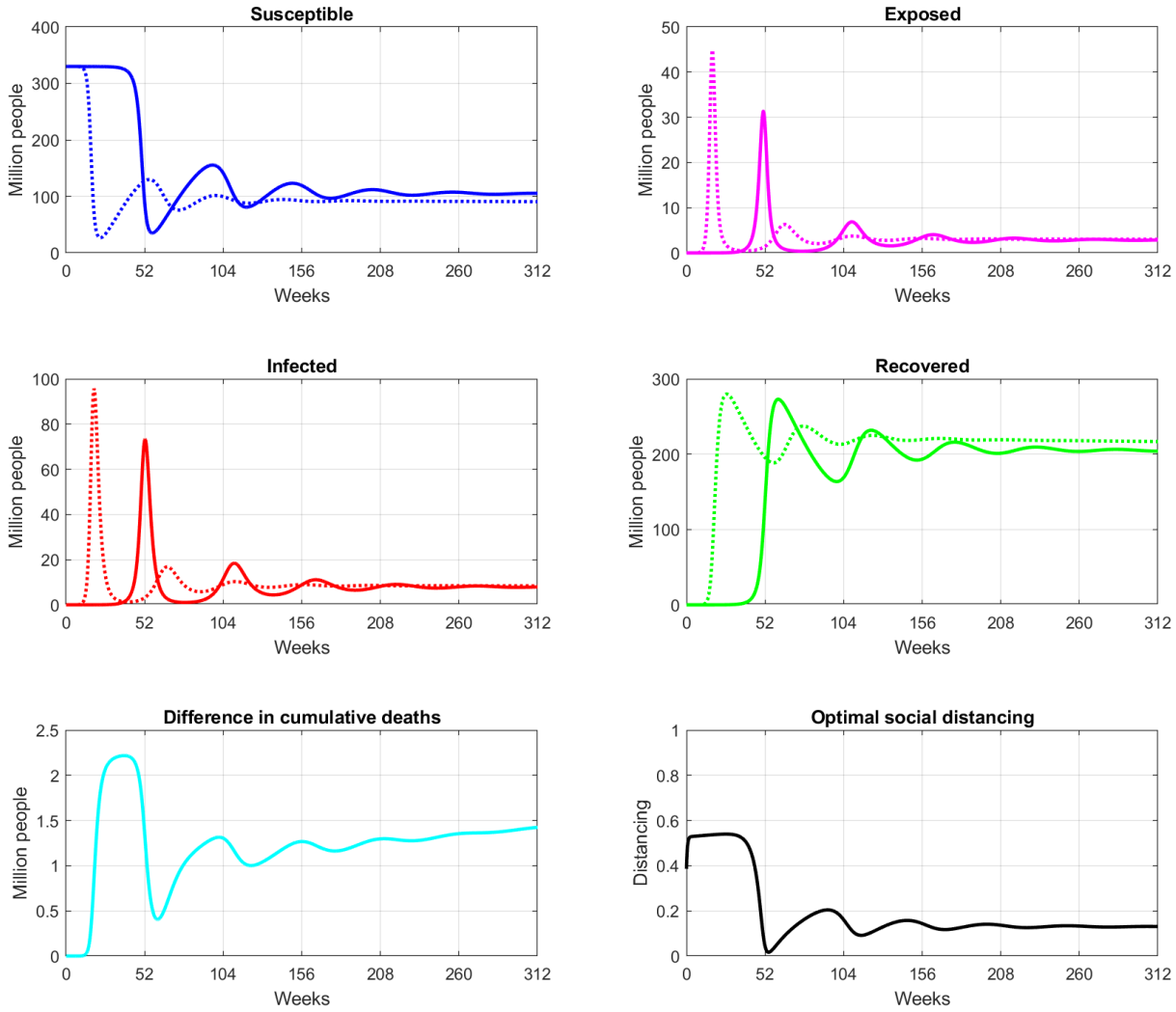

Figure 2: Dynamics for the SEIRS model under the benchmark parameterization. Dotted lines: dynamics under uncontrolled (epidemic) model. Solid lines: dynamics under optimal social distancing. Lower left panel: difference in cumulative disease-induced deaths under controlled and uncontrolled dynamics. Lower right panel: optimal social distancing.

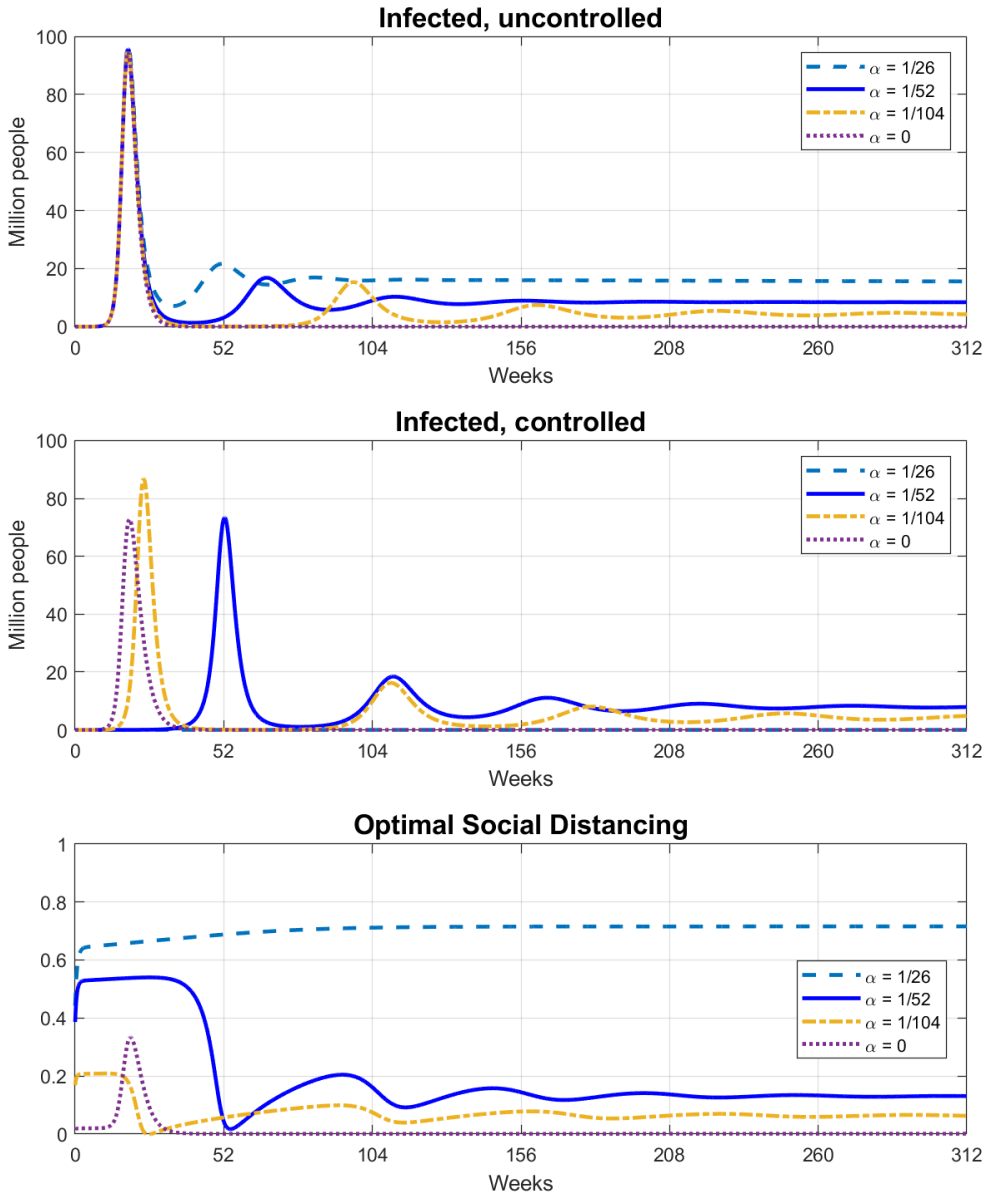

Figure 3: *Sensitivity with respect to the duration of immunity.* Top panel shows the number of infected individuals in the epidemic (uncontrolled) model, middle panel shows the infected for in the optimally controlled model and the bottom panel shows the optimal social distancing policy. All panels are plotted for $1/\alpha = 26,\ 52,\ 104,$ and ∞ weeks.

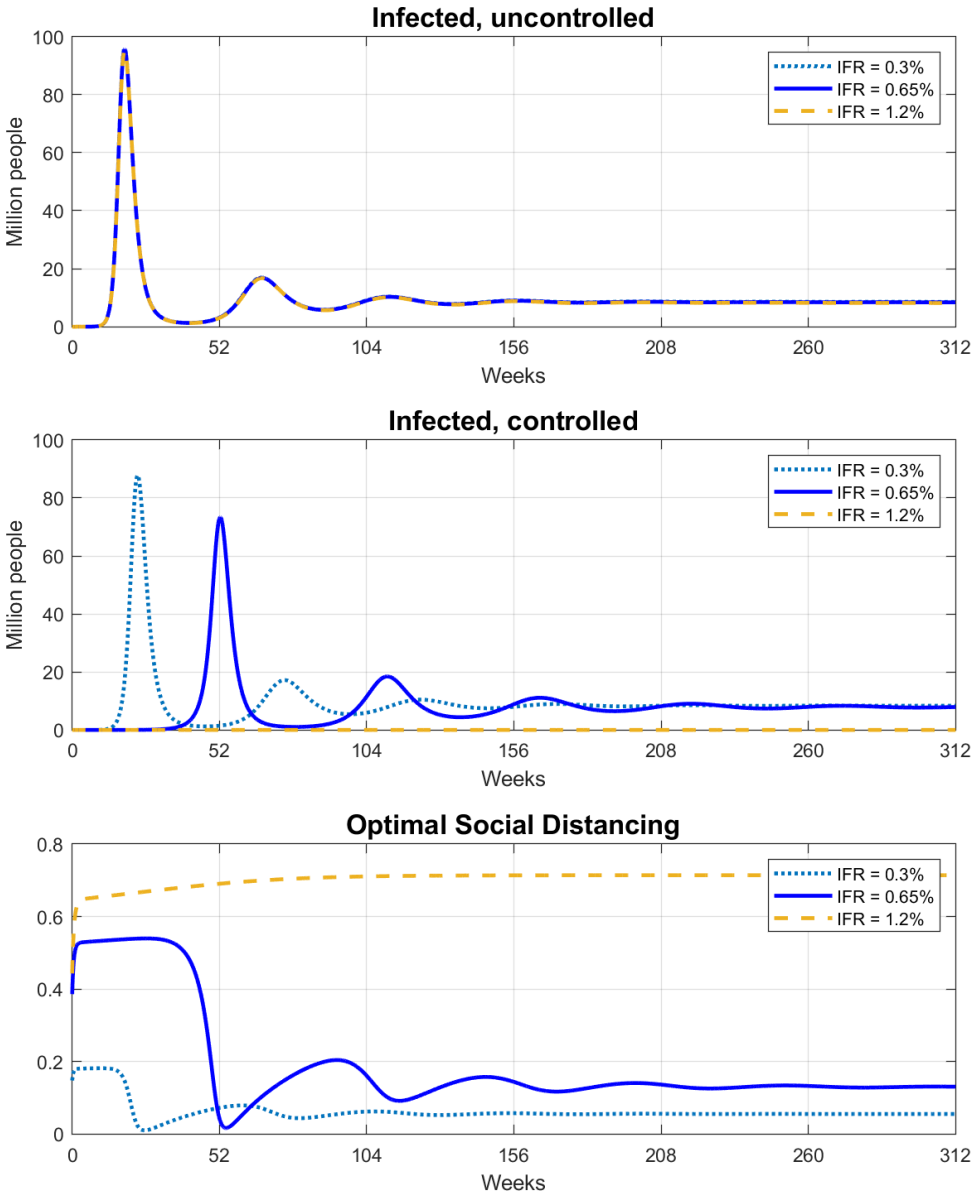

Figure 4: *Sensivity with respect to the infection fatality rate.* Top panel shows the number of infected individuals in the epidemic (uncontrolled) model, middle panel shows the infected in the optimally controlled model and the bottom panel shows the optimal social distancing policy. All panels are plotted for infection fatality rate 0.3%, 0.65% (benchmark) and 1.2%.

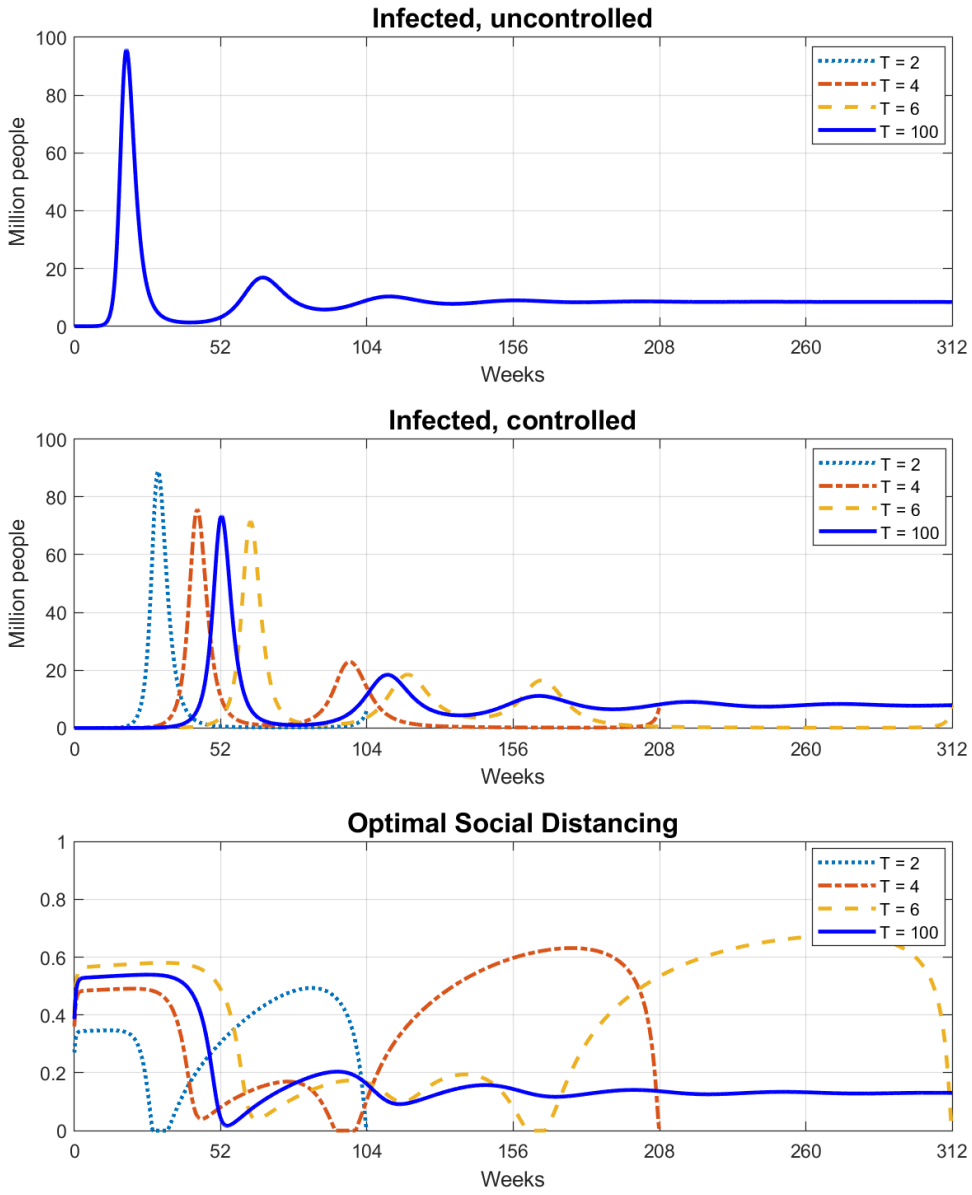

Figure 5: *Sensivity with respect to the planning horizon* T. Top panel shows the number of infected individuals in the epidemic (uncontrolled) model, middle panel shows the infected in the optimally controlled model and the bottom panel shows the optimal social distancing policy. All panels are plotted for planning time horizons $T = 2,\ 4,\ 6$ and 100 years.

WANING IMMUNITY AND THE SECOND WAVE: SOME PROJECTIONS FOR SARS-CoV-2

** ONLINE APPENDIX **

Chryssi Giannitsarou* Stephen Kissler† Flavio Toxvaerd‡

First draft: 2 June 2020;
Current draft: 22 Sep 2020

*Faculty of Economics, University of Cambridge and CEPR. Email: cg349@cam.ac.uk.
†Harvard School of Public Health. Email: skissler@hsph.harvard.edu.
‡Faculty of Economics, University of Cambridge. Email: fmot2@cam.ac.uk.

A. Flow Chart of the SEIRS Model with Demographics

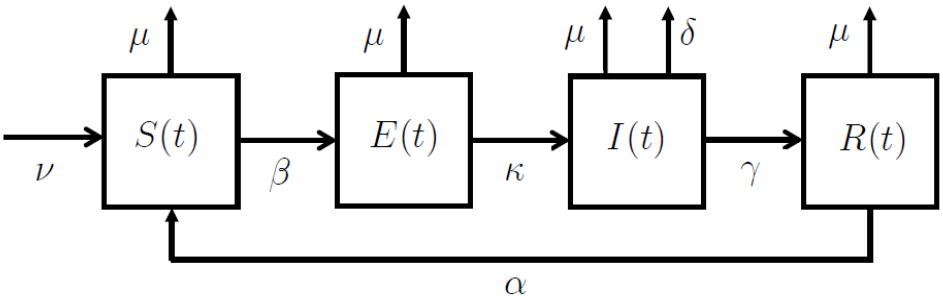

Figure 1: States and flows in the SEIRS model.

B. Tables

Parameter	Value	Source
ν	3.8/52	USA average 3.8 million births per year
μ	$1/(80 \times 52)$	USA life expectancy 80 years
γ	7/14	Kissler et al. (2020)
β	$\gamma \times 3$	Kissler et al. (2020)
κ	7/5	Kissler et al. (2020) and references therein
ε	1/2	Davies et al. (2020)
δ	$\gamma \times 0.0065$	IFR, various sources.
α	1/52	Kissler et al. (2020)
ρ	0.04/52	Standard yearly macro discount rate, 4%
y_S	1	Normalized to 1 unit of income
y_E	1	Equal to y_S
y_I	0.9	10% reduction in productivity due to infection
y_R	1	Equal to y_S
y	1	Income per person after T, equal to y_S
η	1	Quadratic costs
$\theta/2$	330×0.165	Aggregate income loss (Strong and Wellbourn, 2020)
T	100×52	Approximation of long/infinite horizon
N_0	330	US population, 330m
I_0	0.000033	1 in 10 m initially infected, Atkeson (2020)
E_0	$3 \times I_0$	Atkeson (2020)

Table 1: Parameter values for benchmark simulations.

	At the end of 6 years			At the end of horizon T		
$T = 100$ years	*Epi model*	*Econ model*	*Diff*	*Epi model*	*Econ model*	*Diff*
$IFR = 0.30\%,\ \alpha = 1/52$	4.496m	4.338m	158,010	61.744m	60.341m	1.403m
$IFR = 0.65\%,\ \alpha = 1/52$	**9.636m**	**8.212m**	**1.423m**	**123.440m**	**116.670m**	**6.767m**
$IFR = 1.20\%,\ \alpha = 1/52$	17.490m	14,174	17.476m	202.450m	351,920	202.100m
$IFR = 0.65\%,\ \alpha = 1/26$	16.716m	13,561	16.702m	203.141m	346,360	205.790m
$IFR = 0.65\%,\ \alpha = 1/52$	**9.636m**	**8.212m**	**1.423m**	**123.440m**	**116.670m**	**6.767m**
$IFR = 0.65\%,\ \alpha = 1/104$	5.764m	5.516m	248,120	69.296m	67.266m	2.070m
$IFR = 0.65\%,\ \alpha = 0$	2.061m	1.959m	102,120	3.280m	3.067m	213,590
$IFR = 0.65\%,\ \alpha = 1/52$				*Epi model*	*Econ model*	*Diff*
$T = 2$ years				3.852m	2.317m	1.535m
$T = 4$ years				6.784m	3.660m	3.123m
$T = 6$ years				4.496m	4.121m	3.754m

Table 2: Disease induced deaths for different scenarios. The benchmark case is highlighted in bold.

C. Long Run Dynamics of the Epidemic Model

The system of differential equations for the epidemic model is given by:

$$\dot{S} = \nu - \beta \frac{(I + \varepsilon E)\, S}{N} + \alpha R - \mu S, \tag{1}$$

$$\dot{E} = \beta \frac{(I + \varepsilon E)\, S}{N} - (\kappa + \mu)\, E, \tag{2}$$

$$\dot{I} = \kappa E - (\gamma + \delta + \mu)\, I, \tag{3}$$

$$\dot{R} = \gamma I - (\alpha + \mu)\, R, \tag{4}$$

$$\dot{N} = \nu - \mu N - \delta I. \tag{5}$$

We start by describing the basic reproductive rate $\mathcal{R}_0$, i.e. the number of secondary infectives per index case in a (naive) population of susceptibles.[1] Under the assumption that at the start of time the entire population is susceptible, the average number of new infections per infectious individual is determined by the transmission rate times the mean time that the exposed and infected individuals are infectious, i.e. by the following expression:

$$\mathcal{R}_0 = \frac{\kappa}{\kappa + \mu} \frac{\beta}{\gamma + \delta + \mu} + \frac{\varepsilon \beta}{\kappa + \mu}. \tag{6}$$

We note that the basic reproduction rate is independent of the waning immunity parameter α, because this parameter has no effect on how many infectives are generated per infectious individual.

To determine possible long run outcomes, we first note that in a long run steady state where population does not grow, we have that $\nu = \mu N^* + \delta I^*$. The model has two such steady states, the *disease-free steady state* and the *endemic steady state*. These can be recovered analytically as follows:

- **Disease-free steady state**: In this steady state $I^* = 0$ and $E^* = 0$. Then $N^* = \nu/\mu$ and $R^* = 0,\ S^* = \nu/\mu$.

- **Endemic steady state**: We require that $I^* \neq 0$, and assuming $\kappa \neq 0$ and $\alpha + \mu \neq 0$, then

$$E^* = \left(\frac{\gamma + \delta + \mu}{\kappa} \right) I^* \equiv \phi I^*, \tag{7}$$

$$R^* = \left(\frac{\gamma}{\alpha + \mu} \right) I^* \equiv \psi I^*. \tag{8}$$

From the first ODE by setting $\dot{S} = 0$, and substituting in the above we can show that

$$\frac{S^*}{N^*} = \frac{1}{\mathcal{R}_0}. \tag{9}$$

This means that in the endemic steady state of the SEIRS model with demographics (births and deaths), the proportion of susceptibles is inversely proportional to the basic reproduction rate $\mathcal{R}_0$.[2] With these expressions in place we can derive the population at the endemic steady

[1] This definition is taken from Keeling and Rohani (2008).

[2] Similar results can be shown for variations of such models with demographics, as explained in Keeling and Rohani (2008).

state to be

$$N^* = \nu \left(\frac{\delta}{1+\phi+\psi} \left(1 - \frac{1}{\mathcal{R}_0} \right) + \mu \right)^{-1} \tag{10}$$

and the following relations

$$\frac{E^*}{N^*} = \frac{\phi}{1+\phi+\psi} \left(1 - \frac{1}{\mathcal{R}_0} \right), \tag{11}$$

$$\frac{I^*}{N^*} = \frac{1}{1+\phi+\psi} \left(1 - \frac{1}{\mathcal{R}_0} \right), \tag{12}$$

$$\frac{R^*}{N^*} = \frac{\psi}{1+\phi+\psi} \left(1 - \frac{1}{\mathcal{R}_0} \right). \tag{13}$$

To analyze the stability of the two steady states, we derive the Jacobian of the system:

$$J\left(S,E,I,N\right) = \begin{bmatrix} -\beta\frac{(I+\varepsilon E)}{N} - (\alpha+\mu) & -\beta\varepsilon\frac{S}{N} - \alpha & -\beta\frac{S}{N} - \alpha & \beta\frac{(I+\varepsilon E)S}{N^2} - \alpha \\ \beta\frac{(I+\varepsilon E)}{N} & \beta\varepsilon\frac{S}{N} - (\kappa+\mu) & \beta\frac{S}{N} & -\beta\frac{(I+\varepsilon E)S}{N^2} \\ 0 & \kappa & -\kappa\phi & 0 \\ 0 & 0 & -\delta & -\mu \end{bmatrix}. \tag{14}$$

For the disease-free steady state, this becomes

$$J_{DF} = \begin{bmatrix} -(\alpha+\mu) & -\beta\varepsilon - \alpha & -\beta - \alpha & -\alpha \\ 0 & \beta\varepsilon - (\kappa+\mu) & \beta & 0 \\ 0 & \kappa & -\kappa\phi & 0 \\ 0 & 0 & -\delta & -\mu \end{bmatrix} \tag{15}$$

and for the endemic steady state, this becomes

$$J_E = \begin{bmatrix} -\beta\left(\frac{1+\varepsilon\phi}{1+\phi+\psi}\right)\left(1-\frac{1}{\mathcal{R}_0}\right) - (\alpha+\mu) & -\beta\varepsilon\frac{1}{\mathcal{R}_0} - \alpha & -\beta\frac{1}{\mathcal{R}_0} - \alpha & \beta\left(\frac{1+\varepsilon\phi}{1+\phi+\psi}\right)\left(1-\frac{1}{\mathcal{R}_0}\right)\frac{1}{\mathcal{R}_0} - \alpha \\ \beta\left(\frac{1+\varepsilon\phi}{1+\phi+\psi}\right)\left(1-\frac{1}{\mathcal{R}_0}\right) & \beta\varepsilon\frac{1}{\mathcal{R}_0} - (\kappa+\mu) & \beta\frac{1}{\mathcal{R}_0} & -\beta\left(\frac{1+\varepsilon\phi}{1+\phi+\psi}\right)\left(1-\frac{1}{\mathcal{R}_0}\right)\frac{1}{\mathcal{R}_0} \\ 0 & \kappa & -\phi\kappa & 0 \\ 0 & 0 & -\delta & -\mu \end{bmatrix}. \tag{16}$$

It can be shown that whenever $\mathcal{R}_0 < 1$, then the disease-free steady state is stable and the endemic steady state is unstable, while whenever $\mathcal{R}_0 > 1$, the disease-free steady state is unstable and the endemic steady state is stable. We can also confirm numerically that for our calibrated parameters and the ranges of parameters relevant for SARS-CoV-2, the disease-free steady state is unstable (i.e. at least one eigenvalue of J_{DF} has strictly positive real part) , while the endemic steady state is stable (i.e. all eigenvalues of J_E have strictly negative real parts). Importantly this is true for both $\alpha \neq 0$, i.e. for waning immunity and for $\alpha = 0$, i.e. for the SEIR model, for which immunity of individuals is permanent. Additionally, the endemic steady state exhibits damped oscillations (again irrespective of α), because J_E has eigenvalues that are conjugate complex.

The figures that follow show the uncontrolled disease dynamics in the following cases for short and long horizons for permanent immunity $\alpha = 0$ (Figure 2) and waning immunity $\alpha = 1/52$ (Figure 3). For all these, the initial condition of the population has now been set to the disease-free steady state $N^* = 304$ million people.

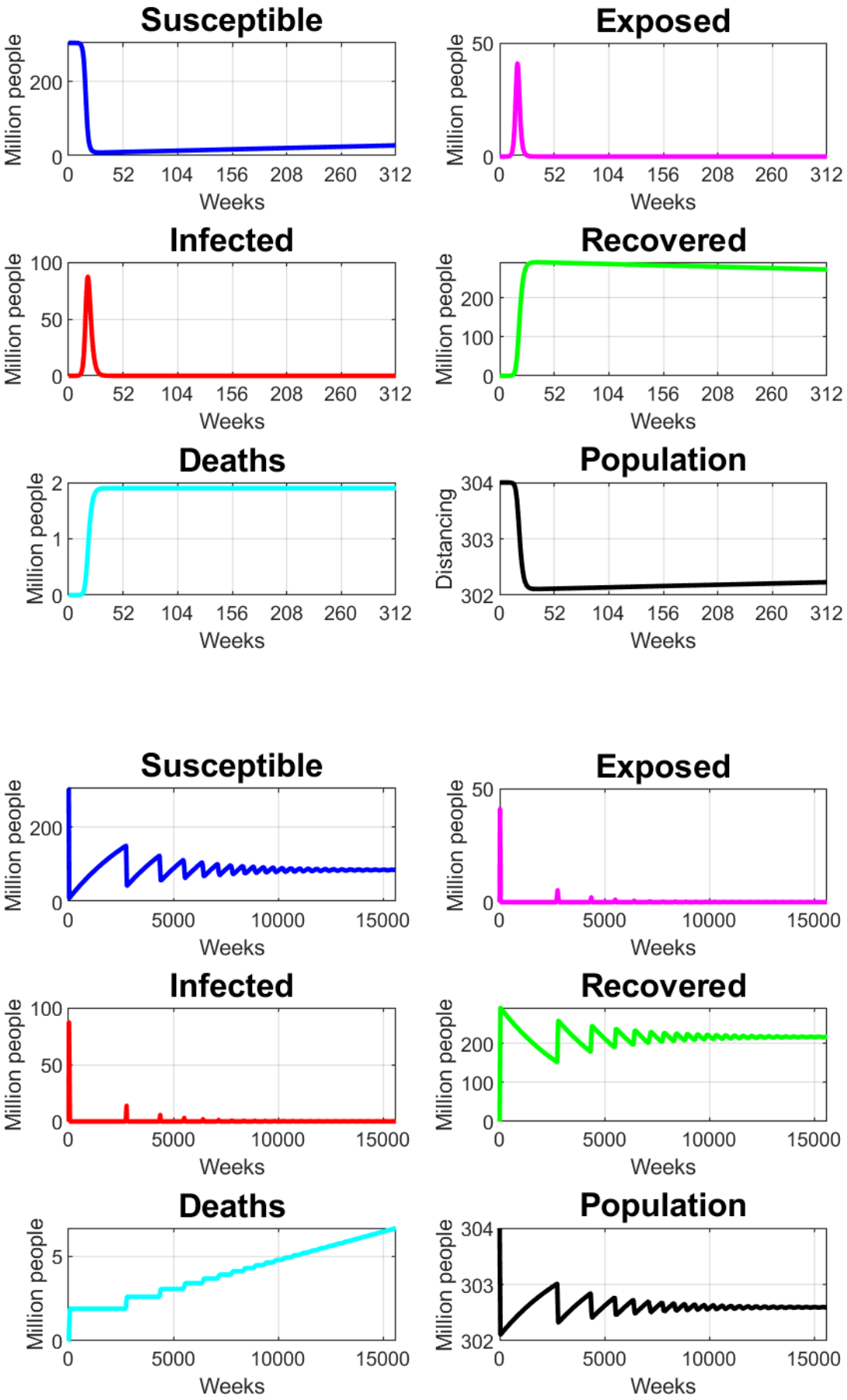

Figure 2: SEIR with demographics, uncontrolled dynamics. Top three rows show first six years, bottom three rows 300 years.

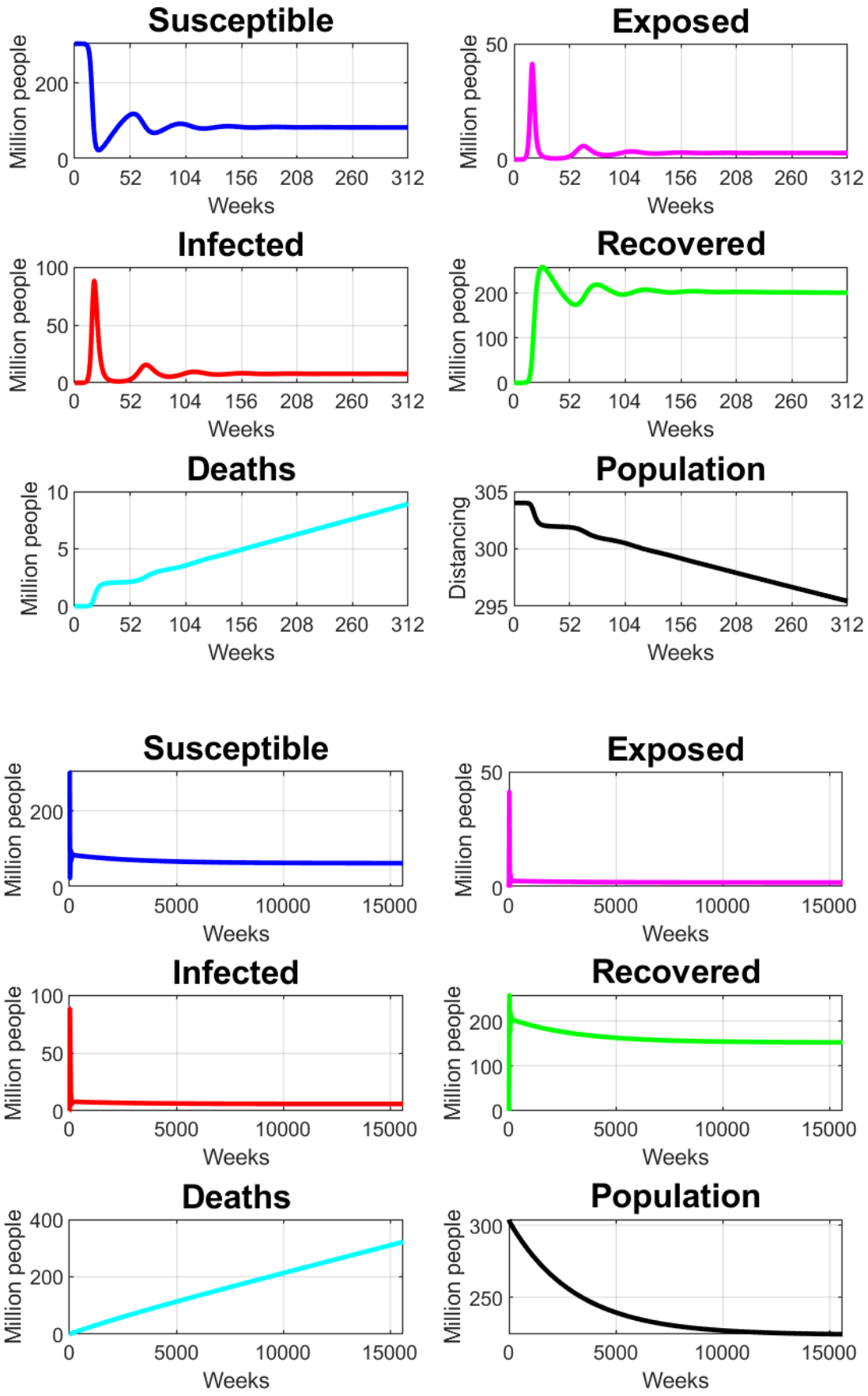

Figure 3: SEIRS with demographics, uncontrolled dynamics ($\alpha = 1/52$). Top three rows show first six years, bottom three rows 300 years.

D. Infectivity Reductions in the Epidemic Model

In the main analysis, we interpret the policy instrument d as some measure that reduces contacts between at-risk individuals and infectious individuals and we allow the social planner to vary this instrument at will over time. It is instructive to consider the dynamics of the model with some fixed value of d, which can be interpreted as other measures which reduce the infectiousness of the disease. For example, mass vaccination with incomplete vaccination coverage or with vaccines that only confer partial protection (as is the case with many vaccines) would effectively reduce the infectiousness parameter of the disease below the level β in such a manner.

Let the epidemic model now be described by

$$\dot{S} = \nu - (1-d)\beta\frac{(I+\varepsilon E)\,S}{N} + \alpha R - \mu S, \tag{17}$$

$$\dot{E} = (1-d)\beta\frac{(I+\varepsilon E)\,S}{N} - (\kappa+\mu)\,E, \tag{18}$$

$$\dot{I} = \kappa E - (\gamma+\delta+\mu)\,I, \tag{19}$$

$$\dot{R} = \gamma I - (\alpha+\mu)\,R, \tag{20}$$

$$\dot{N} = \nu - \mu N - \delta I, \tag{21}$$

where here we think of $d \in [0,1]$ as a *constant* parameter. The interpretation is the same as in the main part of the paper, i.e. that d is a way of reducing the contact rate between susceptibles and infectious individuals (exposed and infected) and can be loosely interpreted as a measure of social distancing. In this version of the model, the basic reproductive rate is given by

$$\tilde{\mathcal{R}}_0 = \frac{\kappa}{\kappa+\mu}\frac{\beta\,(1-d)}{\gamma+\delta+\mu} + \frac{\varepsilon\beta\,(1-d)}{\kappa+\mu}. \tag{22}$$

There are again two steady states, one endemic and one disease-free, and only one of them can be stable for each set of parameters. Specifically, if $\tilde{\mathcal{R}}_0 > 1$, then the endemic steady state is stable, while when $\tilde{\mathcal{R}}_0 < 1$ the disease-free steady state is stable. To link this with the original epidemic model, we note that the condition for the disease-free steady state to be stable is equivalent to requiring that

$$d > 1 - \frac{1}{\mathcal{R}_0} \equiv \tilde{d}, \tag{23}$$

where $\mathcal{R}_0$ is the rate of the basic epidemic model given in (6). This expression is very useful for understanding and interpreting the effects of the optimal social distancing policy: it shows that with enough social distancing (anything above a threshold $\tilde{d}$) it is possible to eradicate an otherwise endemic disease. As will be the case for some extreme parameterizations of the model, the social planner will optimally choose a long run social distancing policy that will be just about enough to tip the dynamics of the system towards the disease-free steady state. For which parameters this happens depends on the optimal control parameters, i.e. the cost of social distancing, the loss of income from those infected, the loss of lives, etc. For our benchmark calibration as given in Table 1, the value of this threshold is $\tilde{d} = 0.7154$.

E. Optimal Social Distancing Policy

The planner's problem is

$$\max_{d\in[0,1]}\left\{\int_0^T \exp\left(-\rho t\right)\left(y_S S\left(t\right)+y_E E\left(t\right)+y_I I\left(t\right)+y_R R\left(t\right)-\frac{\theta}{2}d^2\right)dt \right. \tag{24}$$
$$\left. +\int_T^\infty \exp\left(-\rho t\right) yN(t)dt\right\}.$$

The second integral, which represents the *scrap* or *salvage* value for the optimal control problem, is the integral from time T to infinity of the discounted value of the income generated by the total population, where the dynamics of the population are now determined by the ODE for N, but without the disease induced death rate. We assume that the income produced by each individual after T is y, and it satisfies $y = y_S$. That is,

$$V=\int_T^\infty \exp\left(-\rho t\right) N\left(t\right) y dt. \tag{25}$$

The ODE for population is $\dot{N}=\nu-\mu N$ and therefore its solution is

$$N\left(t\right)=\frac{\nu}{\mu}+C\exp\left(-\mu t\right), \tag{26}$$

where C is the constant to be determined by the size of the population at time T. For $N\left(T\right)$ at the start of the integral we have

$$N\left(T\right)=\frac{\nu}{\mu}+C\exp\left(-\mu T\right) \implies C=\left(N\left(T\right)-\frac{\nu}{\mu}\right)\exp\left(\mu T\right). \tag{27}$$

Therefore after T, the population evolves according to

$$N\left(t\right)=\frac{\nu}{\mu}+\left(N\left(T\right)-\frac{\nu}{\mu}\right)\exp\left(-\mu\left(t-T\right)\right), \text{ for } t\geq T. \tag{28}$$

With this in place we can now derive the scrap value to be

$$\begin{aligned} V &= \int_T^\infty y\exp\left(-\rho t\right)N\left(t\right)dt && (29)\\ &= \int_T^\infty y\exp\left(-\rho t\right)\left[\frac{\nu}{\mu}+\left(N\left(T\right)-\frac{\nu}{\mu}\right)\exp\left(\mu T\right)\exp\left(-\mu t\right)\right]dt && (30)\\ &= \exp\left(-\rho T\right)\left[\frac{\nu}{\rho\mu}+\left(N\left(T\right)-\frac{\nu}{\mu}\right)\frac{1}{\rho+\mu}\right]y. && (31)\end{aligned}$$

Therefore, the problem of the planner can be rewritten as

$$\max_{d\in[0,1]}\left\{\int_0^T \exp\left(-\rho t\right)\left(y_S S+y_E E+y_I I+y_R R-\frac{\theta}{2}d^2\right)dt \right. \tag{32}$$
$$\left. +\exp\left(-\rho T\right)\left[\frac{\nu}{\rho\mu}+\frac{1}{\rho+\mu}\left(N\left(T\right)-\frac{\nu}{\mu}\right)\right]y\right\}.$$

We start with the five differential equation constraints that describe the dynamics of the system:

$$\dot{S} = \nu - (1-d)\beta\left(I + \varepsilon E\right)\frac{S}{N} + \alpha R - \mu S, \tag{33}$$

$$\dot{E} = (1-d)\beta\left(I + \varepsilon E\right)\frac{S}{N} - (\kappa + \mu)\, E, \tag{34}$$

$$\dot{I} = \kappa E - (\gamma + \delta + \mu)\, I, \tag{35}$$

$$\dot{R} = \gamma I - (\alpha + \mu)\, R, \tag{36}$$

$$\dot{N} = \nu - \mu N - \delta I. \tag{37}$$

Because of the accounting equation, the social planner's problem can be reduced to one with only four differential equation constraints. We do so by eliminating R and substituting in $R = N - S - E - I$. The constraints thus become

$$\dot{S} = \nu + \alpha N - (\alpha + \mu)\, S - \alpha E - \alpha I - (1-d)\beta\left(I + \varepsilon E\right)\frac{S}{N}, \tag{38}$$

$$\dot{E} = (1-d)\beta\left(I + \varepsilon E\right)\frac{S}{N} - (\kappa + \mu)\, E, \tag{39}$$

$$\dot{I} = \kappa E - (\gamma + \delta + \mu)\, I, \tag{40}$$

$$\dot{N} = \nu - \mu N - \delta I. \tag{41}$$

Letting the costate variables for the constraints be denoted by λ_S, λ_E, λ_I and λ_N, the planner's Hamiltonian is given by

$$\begin{aligned} H \;=\; & e^{-\rho t}\left[\left(y_S - y_R\right) S + \left(y_S - y_R\right) E + \left(y_I - y_R\right) I + y_R N - \frac{\theta}{2} d^2\right] \\ & + \lambda_S\left[\nu + \alpha N - (\alpha + \mu)\, S - \alpha E - \alpha I - (1-d)\beta\left(I + \varepsilon E\right)\frac{S}{N}\right] \\ & + \lambda_E\left[(1-d)\beta\left(I + \varepsilon E\right)\frac{S}{N} - (\kappa + \mu)\, E\right] + \lambda_I\left[\kappa E - (\gamma + \delta + \mu)\, I\right] \\ & + \lambda_N\left(\nu - \mu N - \delta I\right). \end{aligned} \tag{42}$$

The first order condition with respect to d is

$$\frac{\partial H}{\partial d} = -e^{-\rho t}\theta d + \left(\lambda_S - \lambda_E\right)\beta\left(I + \varepsilon E\right)\frac{S}{N} = 0, \tag{43}$$

and therefore the optimal d must satisfy

$$d = \frac{e^{\rho t}}{\theta}\left(\lambda_S - \lambda_E\right)\beta\left(I + \varepsilon E\right)\frac{S}{N}. \tag{44}$$

Additionally, the optimal d^* must belong to the set of admissible controls, and since it is bounded and must satisfy $0 \leq d \leq 1$, it follows that:

$$d^* = \max\left\{0, \min\left\{1, \frac{e^{\rho t}}{\theta}\left(\lambda_S - \lambda_E\right)\beta\left(I + \varepsilon E\right)\frac{S}{N}\right\}\right\}. \tag{45}$$

A detailed explanation and derivations of how the maximum principle applies to bounded controls can be found in Lenhart and Workman (2007, ch. 7).

The laws of motion for the costate variables are given by

$$\dot{\lambda}_S = \lambda_S \left[\beta(1-d)\frac{(I+\varepsilon E)}{N} + \alpha + \mu\right] - \lambda_E \beta(1-d)\frac{(I+\varepsilon E)}{N} - e^{-\rho t}\left(y_S - y_R\right), \tag{46}$$

$$\dot{\lambda}_E = \lambda_S \left[\alpha + \beta\varepsilon(1-d)\frac{S}{N}\right] + \lambda_E \left[\kappa + \mu - (1-d)\beta\varepsilon\frac{S}{N}\right] - \kappa\lambda_I - e^{-\rho t}\left(y_S - y_R\right), \tag{47}$$

$$\dot{\lambda}_I = \left[\alpha + \beta\left(1-d\right)\frac{S}{N}\right)\right]\lambda_S - \beta(1-d)\frac{S}{N}\lambda_E + \left(\gamma + \delta + \mu\right)\lambda_I + \lambda_N\delta - e^{-\rho t}\left(y_I - y_R\right), \tag{48}$$

$$\dot{\lambda}_N = -\lambda_S\alpha - \lambda_S(1-d)\beta\left(I+\varepsilon E\right)\frac{S}{N^2} + \lambda_E(1-d)\beta\left(I+\varepsilon E\right)\frac{S}{N^2} + \mu\lambda_N - e_R^{-\rho t}y_R. \tag{49}$$

Last, we also need the following transversality conditions to be satisfied:

$$\lambda_S\left(T\right) = \lambda_E\left(T\right) = \lambda_I\left(T\right) = 0 \tag{50}$$

and the last transversality condition equates λ_N to the derivative with respect to $N(T)$ of the term

$$\int_T^\infty e^{-\rho t}N(t)ydt = \exp\left(-\rho T\right)\left[\frac{\nu}{\rho\mu} + \frac{1}{\rho+\mu}\left(N\left(T\right) - \frac{\nu}{\mu}\right)\right]y. \tag{51}$$

This yields

$$\lambda_N\left(T\right) = \exp\left(-\rho T\right)\frac{y}{\rho+\mu}. \tag{52}$$

We should point out that the conditions (43), (46), (47), (48), (49), (50) and (52) are necessary for optimality but not sufficient. This stems from the fact that the Hamiltonian (42) is non-concave in the state variables. For this type of problem, neither Mangasarian nor Arrow type sufficiency conditions apply and alternative methods must be used to verify the optimality of a given candidate path.[3] These typically rely on characterizing paths that satisfy the necessary conditions in a neighborhood of multiple steady states and then directly computing and comparing value functions for any regions of the state space in which those multiple paths overlap. In our simulations, we characterize the trajectory of state and costate variables that satisfies the necessary Hamiltonian and transversality conditions. As we have shown, for every parametrization the model exhibits two steady states, of which only one is stable. Moreover, for the parameterizations that we have worked with, we have found no instances of multiple equilibrium paths that satisfy the necessary conditions for optimality.

F. Numerical Solution Method

To solve the model numerically, we use a forward-backward sweep method as described in detail in Lenhart and Workman (2007, ch. 4 and 12). We outline the method here and provide the details of the numerical setup used for generating the figures in the paper.

First, the time interval $[0, T]$ is split into equal intervals each of which has length $h < 1$, and using this time gird of $M+1$ points, the continuous time state and costate variables are approximated with vectors of length $M+1$. The algorithm for finding the optimal policy involves the following steps:

- **Step 1**: Set initial guess for $[d_1, ..., d_{M+1}]$, typically set to zeros.

[3] Brock and Dochert (1983) introduced the generalized maximum principe in the context of growth models, while Brock and Starrett (2003) applied this technique to shallow lake systems. Deissenberg et al. (2004) contains an excellent synthesis of this literature. Rowthorn and Toxvaerd (2020) apply these techniques to the optimal control of disease dynamics.

- **Step 2**: Use initial conditions for $N_1 \equiv N(0)$, $S_1 \equiv S(0)$, $E_1 \equiv E(0)$ and $I_1 \equiv I(0)$ as determined by the model calibration and solve forward in time the system of differential equations (38)-(41), using a 4th order Runge-Kutta forward sweep.

- **Step 3**: Use the transversality conditions (50) and (52), i.e. the costates evaluated at time T, the current vector of d, and the vector of state variables from Step 2, to solve backward in time the system of differential equations (46)-(49), using a 4th order Runge-Kutta backward sweep.

- **Step 4**: Use the current vector of states (from Step 2) and costates (from Step 3) to evaluate d_{new} using (45). Update d using a convex combination of the old and new d, using an updating 'gain' parameter $0 < g < 1$:

$$d = g * d_{new} + (1 - g) * d_{old} \tag{53}$$

- **Step 5**: Iterate until convergence according to a required tolerance level $toler$.

Our results and graphs were generated using the following specifications: First, we use $h = 1/10$. For the smallest time interval we work with, i.e. $T = 104$ weeks, this implies a grid of more than 1,000 points, which is sufficient for a good approximation. We have also tried values of $h = 1/50$ and $h = 1/100$ and found that the improvements in precision are insignificant. Since a larger number of grid points greatly increases computational time, we kept $1/10$ as our benchmark value for h.

Second, we use an updating gain parameter of $g = 0.01$ for almost all simulations, apart from a few simulations with high δ, or high α, and/or large (approximately infinite) time T. The smallest updating gain we used was $g = 0.0005$. Smaller gain improves the stability of the algorithm, but increases the computing time considerably.

Third, for the convergence of the '*while*' loop we use tolerance level $tol = 1e-13$. Requiring tight tolerance for the numerical simulations is very important for good accuracy of the algorithm because of the control bounds. If the tolerance is wide, then the algorithm may 'converge' too quickly and produce solutions that are on the lower or upper bound of the control (i.e. at 0 or 1) for most of the time horizon, and which are *not* optimal.

Fourth, for most of our simulations, our approximation of a very long horizon is done by setting $T = 100$ years. For 'infinite' horizon approximations we discard the last 200-400 weeks to avoid end-of-horizon distortions. The Matlab code for the simulations is provided on the corresponding author's website.

G. Optimal Social Distancing in SEIR Without Demographics

The following two figures show the dynamics and optimal policy for the SEIR model (i.e. permanent immunity) in (a) the benchmark case, i.e. with natural births and deaths, and (b) in a version without demographics, i.e. $\nu = \mu = 0$, both showing the first six years of simulations for $T = 100$ years. We note that the main differences between these sets of plots are quantitative rather than qualitative. Notably, optimal social distancing is significantly higher when a closed population is considered. Intuitively, when the population is not replenished by new births, each individual life receives a much higher weight in the planner's objective and hence there is a much stronger need to avoid infections. Disregarding demographics may thus lead to policy recommendations that inflate the need for disease control, relative to the model with population turnover.

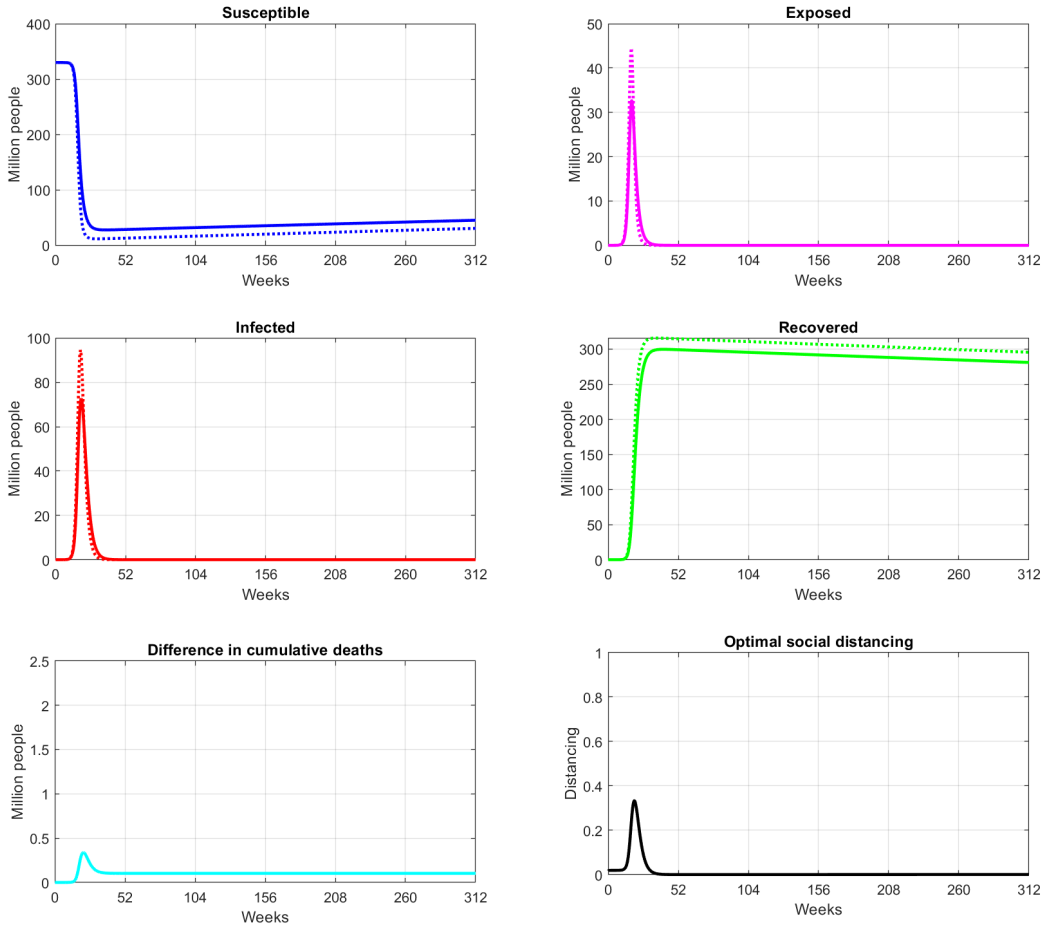

Figure 4: *SEIR model with demographics.* Benchmark values 3.8 million births per year and life expectancy of 80 years. Dotted line is uncontrolled (epidemic) model and solid line under optimal social distancing policy.

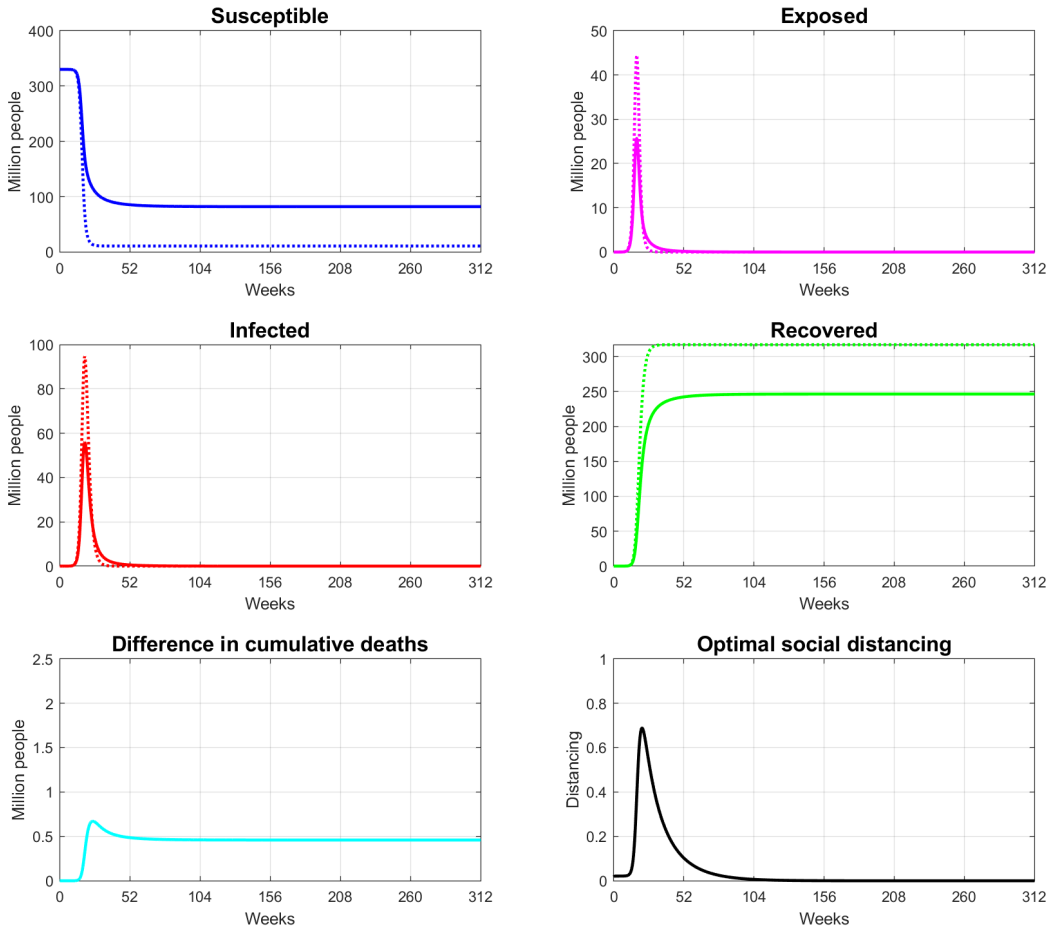

Figure 5: *SEIR model without demographics* ($\nu = \mu = 0$). Dotted line is uncontrolled (epidemic) model and solid line under optimal social distancing policy.

References

[1] Alvarez, F., D. Argente and F. Lippi (2020). A Simple Planning Problem for COVID-19 Lockdown, *NBER Working Paper* 26981.

[2] Armstrong, Gregory L., Laura A. Conn and Robert W. Pinner (1999). Trends in Infectious Disease Mortality in the United States During the 20th Century, *Journal of the Americal Medical Association*, 281(1), 61-66.

[3] Atkeson, A. (2020). What Will Be the Economic Impact of COVID-19 in the US? Rough Estimates of Disease Scenarios, *NBER Working Paper* 26867.

[4] Brauer, F. and C. Castillo-Chavez (2012). Mathematical Model in Population Biology and Epidemiology, *Springer*.

[5] Brock, W. A. and D. Starrett (2003): Managing Systems with Non-convex Positive Feedback, *Environmental and Resource Economics*, 26(4): 575-602.

[6] Brock, W. A. and W. D. Dochert (1983). The Generalized Maximum Principle, *Social Systems Research Institute Workshop Series*, University of Wisconsin.

[7] Callow, K. A., H. F. Parry, M. Sergeant and D. A. Tyrrell (1990). The Time Course of the Immune Response to Experimental Coronavirus Infection of Man, *Epidemiology and Infection*, 105(2), 435–446. doi: 10.1017/s0950268800048019.

[8] Davies, N.G., P. Klepac, Y. Liu, et al. (2020). Age-Dependent Effects in the Transmission and Control of COVID-19 Epidemics, *Nature Medicine* 26, 1205-1211. https://doi.org/10.1038/s41591-020-0962-9.

[9] Davies, N.G., P. Klepac, Y. Liu, K. Prem, M. Jit, CMMID COVID-19 working group, R. M. Eggo (2020). Age-Dependent Effects in the Transmission and Control of COVID-19 Epidemics, unpublished manuscript, medRxiv doi: https://doi.org/10.1101/2020.03.24.20043018.

[10] Deissenberg, C., G. Feichtinger, W. Semmler and F. Wirl (2004). Multiple Equilibria, History Dependence and Global Dynamics in Intertemporal Optimization Problems, in Barnett et al. (2004). Economic Complexity, Non-Linear Dynamics, Multi-Agents Economies, and Learning, International Symposia in Economic Theory and Econometrics, *Elsevier*.

[11] Eichenbaum, M., S. Rebelo and M. Trabrandt (2020). The Macroeconomics of Epidemics, *NBER Working Paper* 26882.

[12] Galanti, M. and J. Shaman (2020). Direct observation of repeated infections with endemic coronaviruses, *Journal of Infectious Diseases*, doi:10.1093/infdis/jiaa392.

[13] Grassly, Nicholas C., Christophe Fraser and Geoffrey P. Garnett (2005). Host Immunity and Synchronized Epidemics of Syphilis Across the United States, *Nature*, 433, 417-421.

[14] Greer, Meredith, Raj Saha, Alex Gogliettino, Chialin Yu and Kyle Zollo-Venecek (2020). Emergence of Oscillations in a Simple Epidemic Model with Demographic Data, *Royal Society Open Science*, 7(1), https://doi.org/10.1098/rsos.191187.

[15] Grenfell, B. T., O. N. Bjørnstad and J. Kappey (2001). Travelling Waves and Spatial Hierarchies in Measles Epidemics, *Nature*, 414, 716-723.

[16] Grenfell, Bryan and Ottar Bjørnstad (2005). Epidemic Cycling and Immunity, *Nature*, 433, 366-367.

[17] Gudbjartsson, D.F., G.L. Norddahl and P. Melsted et al. (2020). Humoral Immune Response to SARS-CoV-2 in Iceland, *The New England Journal of Medicine,* DOI: 10.1056/NEJMoa2026116.

[18] Hall, R. E., C. Jones and P. Klenow (2020). Trading Off Consumption and COVID-19 Deaths. *Federal Reserve Bank of Minneapolis, Quarterly Review*, 42(1).

[19] Hansen, Victoria, Eyal Oren, Leslie K. Dennis and Heidi E. Brown (2016). Infectious Disease Mortality Trends in the United States, 1980-2014, *Journal of the Americal Medical Association*, 316(20), 2149-2151.

[20] Kaplan, G., B. Moll and G. Violante (2020). The Great Lockdown and the Big Stimulus: Tracing the Pandemic Possibility Frontier for the U.S., *CEPR Discussion Paper 15256.*

[21] Keeling, Matt J. and Pejman Rohani (2008). Modeling Infectious Diseases, *Princeton University Press.*

[22] Kissler, S. M., C. Tedijanto, E. Goldstein, Y. H. Grad and M. Lipsitch (2020). Projecting the Transmission Dynamics of SARS-CoV-2 through the Postpandemic Period, *Science*, 368 (6493), 860–686. doi: 10.1126/science.abb5793

[23] Krueger, D., H. Uhlig and T. Xie (2020). Macroeconomic Dynamics and Reallocation in an Epidemic, *NBER Working Paper* 27047.

[24] Lenhart, S. and J. T. Workman (2007). Optimal Control Applied to Biological Models. Mathematical and Computational Biology Series, *Chapman & Hall/CRC*, London.

[25] Li, R., S. Pei, B. Chen, Y. Song, T. Zhang, W. Yang, and J. Shaman (2020). Substantial undocumented infection facilitates the rapid dissemination of novel coronavirus (SARS-CoV-2). Science, 368 (6490), 489-493. doi: 10.1126/science.abb3221

[26] Meyerowitz-Katz, G. and L. Merone (2020). A systematic review and meta-analysis of published research data on COVID-19 infection-fatality rates, medRxiv 2020.05.03.20089854; doi: https://doi.org/10.1101/2020.05.03.20089854.

[27] Mo, H., Zeng, G., Ren, X., Li, H., Ke, C., Tan, Y., Cai, C., Lai, K., Chen, R., Chan-Yeung, M. And Zhong, N. (2006), Longitudinal profile of antibodies against SARS-coronavirus in SARS patients and their clinical significance. *Respirology*, 11: 49-53. doi:10.1111/j.1440-1843.2006.00783.x

[28] Javier Perez-Saez, Stephen A Lauer, Laurent Kaiser, Simon Regard, Elisabeth Delaporte, Idris Guessous, Silvia Stringhini, Andrew S Azman, et al. (2020). Serology-informed estimates of SARS-CoV-2 infection fatality risk in Geneva, Switzerland, *The Lancet Infectious Diseases*, ISSN 1473-3099, https://doi.org/10.1016/S1473-3099(20)30584-3.

[29] Payne, D. C., Iblan, I., Rha, B., et al. (2016). Persistence of Antibodies against Middle East Respiratory Syndrome Coronavirus. *Emerging Infectious Diseases*, 22(10), 1824-1826. https://dx.doi.org/10.3201/eid2210.160706.

[30] Rachel, Łukasz (2020): The Second Wave, *mimeo.*

[31] Rowthorn, R. and F. Toxvaerd (2020). The Optimal Control of Infectious Diseases Via Prevention and Treatment, *Cambridge-INET Working Paper Series* No: 2020/13.

[32] Salje, H., C. Tran Kiem, N. Lefrancq, N. Courtejoie, P. Bosetti, J. Paireau, A. Andronico, N. Hoze, J. Richet, C-L. Dubost, Y. Le Strat, J. Lessler, D. Levy-Bruhl, A. Fontanet, L. Opatowski, P-Y. Boelle, S. Cauchemez (2020). Estimating the burden of SARS-CoV-2 in France, *Science*, 13 May 2020, doi: 10.1126/science.abc3517.

[33] Seow, J., C. Graham, B. Merrick et al. (2020). Longitudinal evaluation and decline of antibody responses in SARS-CoV-2 infection. Unpublished manuscript, medRxiv 2020.07.09.20148429; doi: https://doi.org/10.1101/2020.07.09.20148429.

[34] Strong, A. and J. W. Welburn (2020). An Estimation of the Economic Costs of Social-Distancing Policies, Research Report RR-A173-1, *RAND Corporation.*

[35] Swanson, D. and R. Cossman (2020). A Simple Method for Estimating the Number of Unconfirmed COVID-19 Cases in a Local Area that Includes a Confidence Interval: A Case Study of Whatcom County, Washington, unpublished manuscript, medRxiv, doi: 10.1101/2020.04.30.20086181.

[36] To, K. K. W, I. Fan-Ngai Hung, J. D. Ip, et al. (2020). COVID-19 re-infection by a phylogenetically distinct SARS-coronavirus-2 strain confirmed by whole genome sequencing, *Clinical Infectious Diseases*, https://doi.org/10.1093/cid/ciaa1275.

[37] Toxvaerd, F. (2019). Rational Disinhibition and Externalities in Prevention, *International Economic Review*, 60(4), 1737-1755.

[38] Toxvaerd, F. (2020). Equilibrium social Distancing, *Cambridge-INET Working Paper Series* No: 2020/08.

[39] Verity, R., L. C. Okell, I. Dorigatti, P. Winskill, C. Whittaker, N. Imai, G. Cuomo-Dannenburg, H. Thompson, P. G. T. Walker, H. Fu, A. Dighe, J. T. Griffin, M. Baguelin, S. Bhatia, A. Boonyasiri, A. Cori, Z. Cucunube, R. FitzJohn, K. Gaythorpe, W. Green, A. Hamlet, W. Hinsley, D. Laydon, G. Nedjati-Gilani, S. Riley, S. van Elsland, E. Volz, H. Wang, Y. Wang, X. Xi, C. A. Donnelly, A. C. Ghani, N. M. Ferguson (2020). Estimates of the Severity of Coronavirus Disease 2019: A Model-Based Analysis, *The Lancet Infectious Diseases*, 20(6), 669-677, https://doi.org/10.1016/S1473-3099(20)30243-7.